

UltraLogLog: A Practical and More Space-Efficient Alternative to HyperLogLog for Approximate Distinct Counting

Otmar Ertl

Dynatrace Research

Linz, Austria

otmar.ertl@dynatrace.com

ABSTRACT

Since its invention HyperLogLog has become the standard algorithm for approximate distinct counting. Due to its space efficiency and suitability for distributed systems, it is widely used and also implemented in numerous databases. This work presents UltraLogLog, which shares the same practical properties as HyperLogLog. It is commutative, idempotent, mergeable, and has a fast guaranteed constant-time insert operation. At the same time, it requires 28% less space to encode the same amount of distinct count information, which can be extracted using the maximum likelihood method. Alternatively, a simpler and faster estimator is proposed, which still achieves a space reduction of 24%, but at an estimation speed comparable to that of HyperLogLog. In a non-distributed setting where martingale estimation can be used, UltraLogLog is able to reduce space by 17%. Moreover, its smaller entropy and its 8-bit registers lead to better compaction when using standard compression algorithms. All this is verified by experimental results that are in perfect agreement with the theoretical analysis which also outlines potential for even more space-efficient data structures. A production-ready Java implementation of UltraLogLog has been released as part of the open-source Hash4j library.

1 INTRODUCTION

Many applications require counting the number of distinct elements in a data set or data stream. It is well-known that exact counting needs linear space [5]. However, the space requirements can be drastically reduced, if approximate results suffice. HyperLogLog (HLL) [22] with improved small-range estimation [19, 26, 36, 40, 48] represents the state-of-the-art approximate distinct-count algorithm. It allows distributed counting of up to the order of $2^{64} \approx 1.8 \cdot 10^{19}$ distinct elements with a relative standard error of $1.04/\sqrt{m}$ using only $6m$ bits [26]. Therefore, it is nowadays offered by a big number of data stores as part of their query language (see e.g. documentation of Timescale, Redis, Oracle Database, Snowflake, Microsoft SQL Server, Google BigQuery, Vertica, Elasticsearch, Aerospike, Amazon Redshift, KeyDB, DuckDB, or Dynatrace Grail). Further applications of HLL include query optimization [24, 32], caching [45], graph analysis [8, 35], attack detection [12, 14], network volume estimation [7], or metagenomics [6, 9, 18, 30].

HLL is actually very simple as exemplified in Algorithm 1. It typically consists of a densely packed array of 6-bit registers r_0, r_1, \dots, r_{m-1} [26] where the number of registers m is a power of 2, $m = 2^p$. The choice of the precision parameter p allows trading space for better estimation accuracy. Adding an element requires calculating a 64-bit hash value. p bits are used to choose a register for the update. The number of leading zeros (NLZ) of the remaining $64 - p$ bits are interpreted as a geometrically distributed update

value ≥ 1 with success probability $\frac{1}{2}$, that is used to update the selected register, if its current value is smaller. Estimating the distinct count from the register values is more challenging, but can also be implemented using a few lines of code [19, 22].

The popularity of HLL is based on following advantageous features that make it especially useful in distributed systems:

Speed: Element insertion is a fast and allocation-free operation with a constant time complexity independent of the sketch size. In particular, given the hash value of the element, the update requires only a few CPU instructions.

Idempotency: Further insertions of the same element will never change the state. This is actually a natural property every count-distinct algorithm should support to prevent duplicates from changing the result.

Mergeability: Partial results calculated over subsets can be easily merged to a final result. This is important when data is distributed or processed in parallel.

Reproducibility: The result does not depend on the processing order, which often cannot be guaranteed in practice anyway. Reproducibility is achieved by a commutative insert operation and a commutative and associative merge operation.

Reducibility: The state can be reduced to a smaller state corresponding to a smaller precision parameter. The reduced state is identical to that obtained by direct recording with lower precision. This property allows adjusting the precision without affecting the mergeability with older records.

Estimation: A fast and robust estimation algorithm ensures nearly unbiased estimates with a relative standard error bounded by a constant over the full range of practical distinct counts.

Simplicity: The implementation requires only a few lines of code. The entire state can be stored in a single byte array of fixed length which makes serialization very fast and convenient. Furthermore, add and in-place merge operations do not require any extra memory allocations.

To our knowledge HLL is so far the most space-efficient practical data structure having all these desired properties. Space-efficiency can be measured in terms of the memory-variance product (MVP) [34], which is the relative variance of the (unbiased) distinct-count estimate \hat{n} multiplied by the storage size in bits

$$\text{MVP} := \text{Var}(\hat{n}/n) \times (\text{storage size in bits}),$$

where n is the true distinct count. If the MVP is asymptotically (for sufficiently large distinct counts) a constant specific to the data structure, it can be used for comparison as it eliminates the general inverse dependence of the relative estimation error on the root of the storage size. Most HLL implementations use 6-bit registers [26] to support distinct counts beyond the billion range, resulting

Algorithm 1: Inserts an element with 64-bit hash value $\langle h_{63}h_{62}\dots h_0 \rangle_2$ into a HyperLogLog consisting of $m = 2^p$ ($p \geq 2$) 6-bit registers r_0, r_1, \dots, r_{m-1} with initial values $r_i = 0$.

```

 $i \leftarrow \langle h_{63}h_{62}\dots h_{64-p} \rangle_2$             $\triangleright$  extract register index
 $a \leftarrow \langle \underbrace{0\dots 0}_p h_{63-p}h_{62-p}\dots h_0 \rangle_2$      $\triangleright$  mask register index bits
 $k \leftarrow \text{n}1z(a) - p + 1$                           $\triangleright$  update value  $k \in [1, 65 - p]$ 
 $\triangleright$  function  $\text{n}1z$  returns the number of leading zeros
 $r_i \leftarrow \max(r_i, k)$                              $\triangleright$  update register

```

in a MVP of 6.48 [34]. A recent theoretical work conjectured a general lower bound of 1.98 for the MVP of sketches supporting mergeability and reproducibility [33], which shows the potential for improvement. Many different approaches have been proposed to beat the space efficiency of HLL, but they all sacrificed at least one of the properties listed above.

Lossless compression of HLL can significantly reduce the storage size [17, 28, 37]. Since the compressed state prevents random access to registers as required for insertion, bulking is needed to realize at least amortized constant update times. The required buffer partially cancels out the memory savings. Recent techniques avoid buffering of insertions. The Apache Data Sketches library [2] provides an implementation using 4 bits per register to store the most frequent values relative to a global offset. Out of range values are kept separately in an associative array. Overall, this leads to a smaller MVP but also to a more expensive insert operation. Its runtime is proportional to the memory size in the worst case, because all registers must be updated whenever the global offset is increased. HyperLogLogLog [27] takes this strategy to the extreme with 3-bit registers and achieves a space saving of around 40% at the expense of an insert operation which, except for very large numbers, has been reported to be on average more than an order of magnitude slower compared to HLL [27].

Interestingly, lossless compression of probabilistic counting with stochastic averaging (PCSA) [23], a less-space efficient (when uncompressed) predecessor of HLL also known as FM-sketch, yields a smaller MVP than with HLL [28, 37]. The compressed probability counting (CPC) sketch as part of the Apache Data Sketches library [2] uses this finding. The serialized representation of the CPC sketch achieves a MVP of around 2.31 [3] that is already quite close to the conjectured lower bound of 1.98 [33]. However, the need of bulked updates to achieve amortized constant-time insertions more than doubles the memory footprint which also makes serialization significantly slower than for the original HLL. Similar to all compressed variants of HLL, the insert operation of the CPC sketch takes time proportional to the sketch size in the worst case.

Lossy compression of HLL has also been proposed [46, 47]. However, like other approaches such as HyperBitBit/HyperBit [38], they trade idempotency for less space and are therefore risky to use [33]. In contrast, sacrificing mergeability for less space is of greater practical interest [13, 25, 29]. When the data is not distributed and a merge operation is not actually needed, the MVP of HLL can be reduced by 36% down to 4.16 by martingale also known as historic inverse probability (HIP) estimation [15, 39]. The theoretical limit of MVP for unmergeable sketches is at most 1.63 [34], and is also nearly reached by the serialized representation of the CPC sketch [3]. More practical data structures with in-memory representations

that can be updated in constant time in the worst case are HLL with vectorized counters [10] and the martingale curtain sketch which achieves a MVP of 2.31 [34]. If the processing order is not well-defined, all of these non-mergeable approaches do not support reproducibility either.

The only mergeable data structure we know of that is more space-efficient than HLL while having essentially the same properties, in particular constant-time worst-case updates, is ExtendedHyperLogLog (EHLL) [31]. It extends the HLL registers from 6 to 7 bits to store not only the maximum update value, but also whether there was an update with a value smaller by one. This additional information can be used to obtain more accurate estimates. In particular, the MVP is reduced by 16% to 5.43. The only thing missing to make it really practical is an estimator for small distinct counts. As with the original HLL [22], it was only proposed to switch to the linear probabilistic count estimator [44]. However, this is problematic because the estimation error in the transition region can be large [19, 26]. Nevertheless, EHLL motivated us to generalize its basic idea by extending HLL registers even further.

1.1 Summary of Contributions

We first describe a data structure that generalizes the known data structures HyperLogLog (HLL) [22], ExtendedHyperLogLog (EHLL) [31], and probabilistic counting with stochastic averaging (PCSA) [23]. We derive analytic expressions for the Fisher information and the Shannon entropy as functions of the data structure parameters. Although these expressions reveal even more space-efficient configurations that could be the subject of future research, the focus of this work is on a setting that leads to a very practical data sketch called UltraLogLog (ULL) with a MVP of 4.63 which is 28% below that of HLL. Since the Shannon entropy is also 24% smaller for the same estimation error, ULL is also more compact when using lossless compression. Moreover, our experimental results indicate that standard compression algorithms additionally benefit from the 8-bit register size of ULL.

To extract all the information contained in the ULL sketch, we applied the maximum likelihood (ML) method that achieves an estimation error as theoretically predicted by the Cramér-Rao bound [11]. Alternatively, we present a faster approach (with better worst-case runtime) based on a further generalization of the recently proposed generalized remaining area (GRA) estimator [43]. Even though our theoretical analysis shows a smaller estimation efficiency than the ML estimator, the MVP with a value of 4.94 still corresponds to a 24% reduction compared to HLL. As the GRA estimator, the basic version of our new estimator works only for distinct counts that are neither too small nor too large. Therefore, we developed two additional estimators specific to those ranges that are also easy to evaluate. Using a novel approach, they are seamlessly combined with the basic estimator to cover the full range of distinct count values. We also analyzed martingale estimation, which can be used for non-distributed data, and found that in this case ULL reduces the MVP by 17% to 3.47 compared to HLL.

All theoretically derived estimators were verified by intensive simulations, which all show perfect agreement with the theoretically predicted estimation errors. In particular, we also use a technique that allows verification for distinct counts on the order of

2^{64} , which is not possible using traditional simulations. Finally, we also present the results of speed benchmarks, which show that ULL is similarly fast as HLL.

An implementation of ULL is publicly available as part of the Hash4j open-source Java library at <https://github.com/dynatrace-oss/hash4j>. The source code to reproduce the results presented in this work can be found at <https://github.com/dynatrace-research/ultraloglog-paper>. A version of this paper extended by an appendix with mathematical derivations and proofs is also available [21].

2 METHODOLOGY

We start by introducing a data structure for approximate distinct counting that generalizes HyperLogLog (HLL) [22], ExtendedHyperLogLog (EHLL) [31], and probabilistic counting with stochastic averaging (PCSA) [23]. As those, it consists of m registers which are initially set to zero. For every added element a uniformly distributed hash value is computed. This hash value is used to extract a uniform random register index $i \in [0, m)$ and some geometrically distributed integer value with probability mass function (PMF)

$$\rho_{\text{update}}(k) = (b-1)b^{-k} \quad k \geq 1, b > 1 \quad (1)$$

that is used to update the i -th register. Each register consists of $q+d$ bits. q bits are used to store the maximum update value u_i seen so far. The remaining d bits indicate whether there have been any updates with values $u_i - 1, \dots, u_i - d$, respectively. Obviously, this update procedure is idempotent meaning that further occurrences of the same elements will never change any register state. As a consequence, the final state of this data structure can be used to estimate the number of inserted distinct elements n .

Every register state can be described by an integer value r_i from $\{0, 1, \dots, 2^{q+d} - 1\}$. We assume that the most significant q bits of r_i are used to store u_i , which can therefore be simply obtained by $u_i = \lfloor \frac{r_i}{2^d} \rfloor$. As example for $q = 6$ and $d = 2$, $r_i = \langle 00011010 \rangle_2$ would mean that the largest update value was $u_i = \langle 000110 \rangle_2 = 6$. The right-most d bits indicate that the register was also already updated with a value of 5 but not yet with 4. If the register gets further updated with value 8, the state would become $r_i = \langle 00100001 \rangle_2$ where the first $q = 6$ bits encode $u_i = \langle 001000 \rangle_2 = 8$ and the left-most $d = 2$ bits indicate that there was no update with value 7 but one with 6. Information about smaller update values is lost. If $u_i \leq d$, there are only $u_i - 1$ smaller update values and therefore only $u_i - 1$ of the d extra bits are relevant and some values like $r_i = \langle 00001001 \rangle_2$ for $q = 6$ and $d = 2$ cannot be attained. Enumerating just possible states would lead to a slightly more compact encoding. However, for the sake of simplicity and also to avoid special cases, we refrain from this small improvement.

In practice, the number of registers m is usually some power of 2, $m = 2^p$ with p being the precision parameter. In this way, a uniform random register index can be chosen by just taking p bits from the hash value. Furthermore, the parameter b is often 2 such that the update value k can be easily obtained from the number of leading zeros (NLZ) of the remaining hash bits and therefore usually requires just a single CPU instruction. Obviously, the cases $b = 2$, $d = 0$ and $b = 2$, $d = 1$ correspond to HLL and EHLL, respectively. Furthermore, since PCSA effectively keeps track of any update values, the stored information corresponds to our generalized data

structure with $b = 2$, $d \rightarrow \infty$. (PCSA typically uses just 64 bits for each register which is sufficient as update values greater than 64 are unlikely for real-world distinct counts.) Another advantage of choosing m as a power of 2 and $b = 2$ is that the data structure can be implemented in such a way that it can later be reduced to a smaller precision parameter p [19]. The result will then be identical as if the smaller precision parameter was chosen from the beginning. This is important for migration scenarios where precision needs to be changed in a way that is compatible and mergeable with historical data.

2.1 Statistical Model

For simplification, we use the common Poisson approximation [19, 22, 43] that the number of inserted distinct elements is not fixed, but follows a Poisson distribution with mean n . As a consequence, since updates are evenly distributed over all registers and the update values are geometrically distributed, the number of updates with value k per register is again Poisson distributed with mean $n\rho_{\text{update}}(k)/m = n(b-1)/(mb^k)$. The probability that a register was updated with value k at least once, denoted by event A_k , is therefore

$$\Pr(A_k) = 1 - z_k \quad \text{with } z_k := e^{-\frac{n(b-1)}{mb^k}}. \quad (2)$$

The probability that u was the largest update value, which implies that there were no updates with values greater than u , is given by $\Pr(A_u \wedge \bigwedge_{k=u+1}^{\infty} \bar{A}_k) = (1 - z_u) \prod_{k=u+1}^{\infty} z_k = z_u^{\frac{1}{b-1}} (1 - z_u)$. The Poisson approximation results in registers that are independent and identically distributed. For the generalized data structure the corresponding probability mass function (PMF) can be written as

$$\rho_{\text{reg}}(r|n) = \Pr(r_i = r) = \quad (3)$$

$$\begin{cases} z_0^{\frac{1}{b-1}} & r=0, \\ z_u^{\frac{1}{b-1}} (1 - z_u) \prod_{j=1}^{u-1} z_{u-j}^{1-l_j} (1 - z_{u-j})^{l_j} & r=u2^d + \langle l_1 \dots l_{u-1} \rangle_2 2^{d+1-u}, 1 \leq u \leq d, \\ z_u^{\frac{1}{b-1}} (1 - z_u) \prod_{j=1}^d z_{u-j}^{1-l_j} (1 - z_{u-j})^{l_j} & r=u2^d + \langle l_1 \dots l_d \rangle_2, d+1 \leq u < w, \\ (1 - z_{w-1}^{\frac{1}{b-1}}) \prod_{j=1}^d z_{w-j}^{1-l_j} (1 - z_{w-j})^{l_j} & r=w2^d + \langle l_1 \dots l_d \rangle_2, \\ 0 & \text{else.} \end{cases}$$

This formula takes into account that update values are limited to the range $[1, w]$. The upper limit is on the one hand a consequence of the number of register bits reserved for storing the maximum update value. If q bits are used, the update values must be truncated at $2^q - 1$ because higher update values cannot be stored. On the other hand, the way the geometrically distributed integer values are typically determined also leads to an upper limit. For example, the update values in Algorithm 1 do not exceed $65 - p$, which results from extracting the update value and the register index from a single 64-bit hash value.

For our theoretical analysis, we consider a simplified model. We assume that registers are initially set to $-\infty$ and that there are no restrictions on the update values. In particular, there are also updates with non-positive values $k \leq 0$ with corresponding (virtual) events A_k occurring with probabilities according to (2). Then the PMF for a register simplifies to

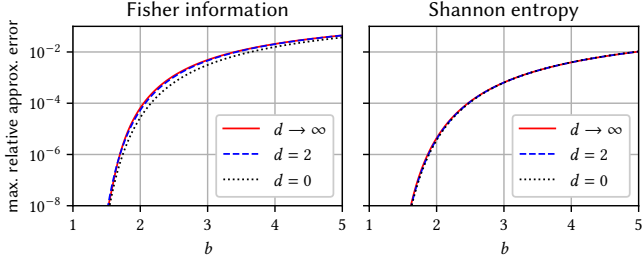


Figure 1: Maximum relative approximation errors of the Fisher information \mathcal{I} and the Shannon entropy \mathcal{H} over b for various values of d .

$$\tilde{\rho}_{\text{reg}}(r|n) = \Pr(r_i = r) = z_u^{\frac{1}{b-1}} (1 - z_u) \prod_{j=1}^d z_{u-j}^{1-l_j} (1 - z_{u-j})^{l_j} \quad \text{with } r = u2^d + \langle l_1 \dots l_d \rangle_2. \quad (4)$$

If all register values are in the range $[(d+1)2^d, w2^d]$, which is usually the case for not too small and not too large distinct counts, (3) and (4) are equivalent. Therefore, the following theoretical results will also hold for (3) when the distinct count is in the intermediate range.

2.2 Theoretical Analysis

Given the register states r_0, \dots, r_{m-1} , the log-likelihood function can be expressed as

$$\ln \mathcal{L} = \ln \mathcal{L}(n|r_0, \dots, r_{m-1}) = \sum_{i=0}^{m-1} \ln \rho_{\text{reg}}(r_i|n). \quad (5)$$

When assuming the simplified PMF (4), the Fisher information can be written as (see Lemma 4 in Appendix A)

$$\mathcal{I} = \mathbb{E} \left(-\frac{\partial^2}{\partial n^2} \ln \mathcal{L} \right) \approx \frac{m}{n^2} \frac{1}{\ln b} \zeta \left(2, 1 + \frac{b^{-d}}{b-1} \right) \quad (6)$$

using the Hurwitz zeta function

$$\zeta(x, y) := \sum_{u=0}^{\infty} (u+y)^{-x} = \frac{1}{\Gamma(x)} \int_0^{\infty} \frac{z^{x-1} e^{-yz}}{1-e^{-z}} dz$$

where $\Gamma(x) := \int_0^{\infty} y^{x-1} e^{-y} dy$ is the gamma function. The approximation in (6) is based on the fact that the Fisher information is a periodic function of $\log_b n$ with period 1 and tiny relative amplitude that can be ignored in practice (see Lemma 2 in Appendix A). The numerical evaluations presented in Figure 1 indicate that the maximum relative approximation error of the Fisher information with respect to the mean is smaller than 10^{-4} for any d and $b \leq 2$, and vanishes as $b \rightarrow 1$. Formula (6) matches the results reported for the special cases of generalized HLL ($d = 0$) and generalized PCSA ($d \rightarrow \infty$) [33].

According to Cramér-Rao [11] the reciprocal of the Fisher information \mathcal{I} is a lower bound for the variance of any unbiased estimator. Our experiments will show that for a sufficiently large number of registers m , this lower bound can be actually reached using maximum likelihood (ML) estimation. The corresponding

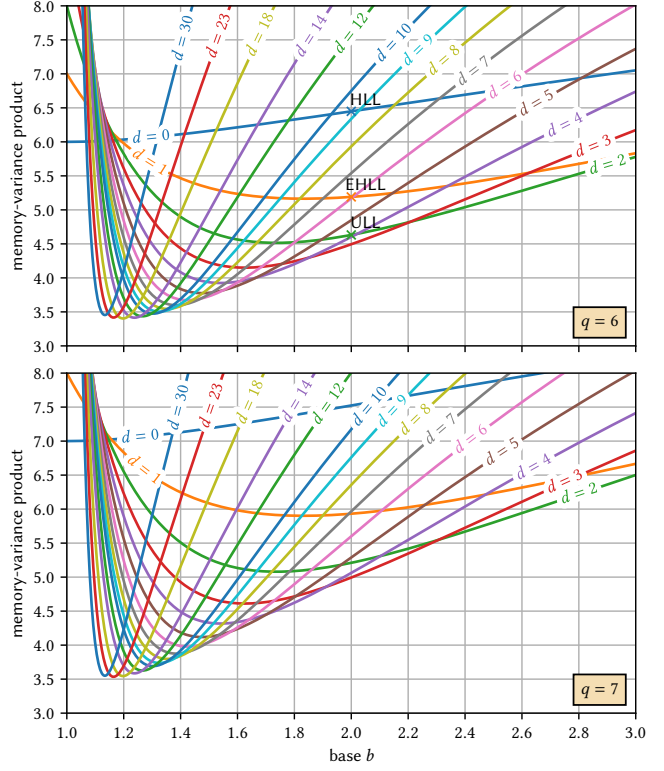


Figure 2: The theoretical asymptotic memory-variance product (MVP) over the base b for $q = 6$ and $q = 7$ and various values of d when assuming a memory footprint of $m(q+d)$ bits. The top chart shows the 28% improvement of UltraLogLog (ULL) over HyperLogLog (HLL).

asymptotic MVP is given by

$$\text{MVP} = m(q+d) \text{Var} \left(\frac{\hat{n}}{n} \right) = \frac{m(q+d)}{\mathcal{I} n^2} \approx \frac{(q+d) \ln b}{\zeta(2, 1 + \frac{b^{-d}}{b-1})}. \quad (7)$$

$(q+d)$ is the number of bits used for a single register. q bits are used for storing the maximum update value and d is the number of extra bits as already described before. The MVP (7) is plotted in Figure 2 over the base b for $q = 6$ and $q = 7$ and various values of d and allows comparing the memory-efficiencies of different configurations, when assuming that the state takes overall $m(q+d)$ bits and is not further compressed.

It is also interesting to compare the MVP for the case, that the state is ideally compressed, which means that the number of bits needed to store the state is given by its Shannon entropy. Considering the resulting MVP, also called Fisher-Shannon (FISH) number, was first proposed in [33]. Using again the simplified PMF (4), the Shannon entropy can be approximated by (see Lemma 5 in Appendix A)

$$\begin{aligned} \mathcal{H} &= \mathbb{E}(-\log_2(\mathcal{L})) \\ &\approx \frac{m}{(\ln 2)(\ln b)} \left(\left(1 + \frac{b^{-d}}{b-1} \right)^{-1} + \int_0^1 z^{\frac{b-d}{b-1}} \frac{(1-z) \ln(1-z)}{z \ln z} dz \right). \end{aligned} \quad (8)$$

Again, we used the same approximation as for the Fisher information, which introduces for the Shannon entropy a relative error smaller than 10^{-5} for all $b \leq 2$ as shown in Figure 1. Combining (6) and (8) gives for the MVP under the assumption of an efficient estimator and optimal compression

$$\text{MVP} = \mathcal{H} \text{Var}\left(\frac{\hat{n}}{n}\right) = \frac{\mathcal{H}}{\mathcal{I} n^2} = \frac{(1 + \frac{b-d}{b-1})^{-1} + \int_0^1 z^{\frac{b-d}{b-1}} \frac{(1-z) \ln(1-z)}{z \ln z} dz}{\zeta(2, 1 + \frac{b-d}{b-1}) \ln 2}. \quad (9)$$

This function is plotted in Figure 3 over the base b for various values of d . The results agree with the conjecture that the MVP of sketches supporting mergeability and reproducibility is fundamentally bounded by $\lim_{\substack{b-d \\ b-1} \rightarrow 0} \frac{\mathcal{H}}{Tn^2} = \frac{1 + \int_0^1 \frac{(1-z) \ln(1-z)}{\zeta(2,1) \ln 2} dz}{\zeta(2,1) \ln 2} \approx 1.98$ [33].

2.3 Choice of Parameters

The data structure proposed in Section 2 has four parameters, the base b , the number of registers $m = 2^p$, the number of register bits q reserved for storing the maximum update value, and the number of additional bits d to indicate the occurrences of the d next smaller update values relative to the maximum. Using the previous theoretical results, we can now find parameters that lead to a small MVP. Here we can essentially leave m aside since it can be used to define the accuracy/space tradeoff, but has essentially no effect on the MVP according to (7) and (9).

The parameters b and q define the operating range of the data structure and must be chosen such that it is very unlikely that all registers get saturated. In other words, the fraction of registers with $r_i \geq w2^d$ must be small. This requires according to (3) that $\Pr(r_i < w2^d) = z^{\frac{1}{b-1}} = \exp(-\frac{n}{mb^{w-1}}) \approx 1$ or $n \ll mb^{w-1}$. Therefore, the maximum supported distinct count n_{\max} can be roughly estimated by $n_{\max} \approx mb^{w-1}$.

If w is limited by the register size ($w = 2^q - 1$, cf. Section 2.1), we get $n_{\max} \approx mb^{2^q-2}$. For HLL with $m = 256$ registers, $b = 2$, and a registers size of $q = 5$ bits, as originally proposed, we have $n_{\max} \approx 275$ billions which might not be sufficient in all situations. For this reason, most HLL implementations use nowadays $q = 6$ [26], which is definitely sufficient for any realistic counts. Some implementations even use a whole byte per register ($q = 8$), but mainly to have more convenient register access in memory [4].

Bearing in mind the operating range defined by m , b , and q , we explore the theoretical MVP (7) for different configurations as shown in Figure 2. First we consider the case $b = 2$ which also covers HLL ($b = 2, d = 0$) and EHLL ($b = 2, d = 1$) and is of particular practical interest due to the very fast mapping of hash values to update values as discussed in Section 2. For $b = 2$, we need to choose $q = 6$, if we want to make sure that any realistic distinct counts can be handled. According to Figure 2 the optimal choice for $b = 2$ would be $d = 3$ resulting in a theoretical MVP of 4.4940. Despite its slightly larger theoretical MVP of 4.6313, the case $d = 2$ is very attractive from a practical point of view since a register takes $q + d = 8$ bits and fits perfectly into a single byte. This enables fast updates as registers can be directly accessed and modified when stored in a byte array. This is why we picked $b = 2, d = 2, q = 6$ as configuration for our new data structure called UltraLogLog (ULL). Its theoretical MVP is 28% smaller than that of HLL with a register

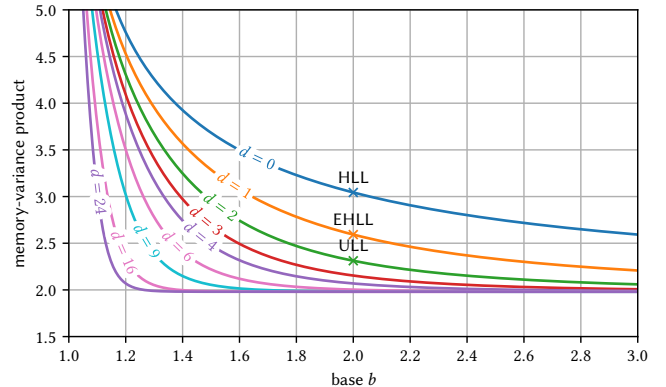


Figure 3: The theoretical asymptotic memory-variance product (MVP) over the base b for various values of d under the assumption of optimal lossless compression. The MVP of UltraLogLog is 24% smaller than that of HyperLogLog.

size of $q = 6$ and a MVP of 6.4485. This even corresponds to a 46% improvement, when compared to HLL implementations that use $q = 8$ bits per register [4] leading to MVP = 8.5981.

Figure 2 shows that the MVP could be further reduced by choosing bases b other than 2. For $q = 6$, a minimum MVP of 3.4030 is achieved for $b = 1.1976$ and $d = 18$. However, a small b leads to a small operating range. For example, $b = 1.1976$ yields $n_{\max} \approx 18$ millions for $m = 256$ which is too small for many applications. However, the working range can be extended again by increasing q . For $q = 7$ the minimum MVP = 3.5338 is obtained for $d = 23$ and $b = 1.1642$ leading to $n_{\max} \approx 53$ billions for $m = 256$. From a practical point of view the configuration $q = 7$, $d = 9$, $b = \sqrt{2}$ with MVP = 3.9025 could be an interesting choice for future research. The operating range would be similar to ULL or HLL, registers would take exactly two bytes ($q + d = 16$), and the mapping of hash values to update values for $b = \sqrt{2}$ according to (1) could be accomplished without expensive logarithm evaluations or table lookups. The update value can be obtained by doubling the number of leading zeros (NLZ) and adding 0 or 1 depending on the remaining hash bits, whose value range is divided into two parts in the ratio $1 : \sqrt{2}$. However, a single 64-bit hash value might not be sufficient in this case.

Figure 3 shows the MVP under the assumption of optimal lossless compression as given by (9). The ULL configuration with $d = 2$ leads to $\text{MVP} = 2.3122$ which is 24% less than for HLL with $d = 0$ and $\text{MVP} = 3.0437$. Therefore, ULL is potentially superior to any variant of HLL that uses lossless compression techniques [2, 27], if similar techniques are also applied to ULL.

The theoretical results show clearly that ULL encodes distinct count information, uncompressed and compressed, more efficiently than HLL. However, an open question is whether this information can also be readily accessed using a simple and robust estimation procedure, which will be the focus of the following sections.

2.4 Maximum-Likelihood Estimator

Since we know the probability mass function (PMF) (3) when using the Poisson approximation, we can simply use the maximum

likelihood (ML) method. For $b = 2$, the log-likelihood function (5) has the shape

$$\ln \mathcal{L} = -\frac{n}{m} \alpha + \sum_{u=1}^{w-1} \beta_u \ln(1 - e^{-\frac{n}{m^{2u}}}),$$

where for ULL with $d = 2$ the coefficients α and β_u are given by

$$\alpha = c_0 + \frac{c_4 + 3c_8 + c_{10}}{4} + \left(\sum_{u=3}^{w-1} \frac{7c_{4u} + 3c_{4u+1} + 5c_{4u+2} + 2c_{4u+3}}{2^u} \right) + \frac{3c_{4w} + c_{4w+1} + 2c_{4w+2}}{2^{w-1}},$$

$$\beta_u = \begin{cases} c_4 + c_{10} + c_{13} + c_{15} & u=1, \\ c_8 + c_{10} + c_{14} + c_{15} + c_{17} + c_{19} & u=2, \\ c_{4u} + c_{4u+1} + c_{4u+2} + c_{4u+3} + c_{4u+6} + c_{4u+7} + c_{4u+9} + c_{4u+11} & 3 \leq u \leq w-2, \\ c_{4w-4} + c_{4w-3} + c_{4w-2} + c_{4w-1} + c_{4w} + c_{4w+1} + 2c_{4w+2} + 2c_{4w+3} & u=w-1, \end{cases}$$

and $c_j := |\{i | r_i = j\}|$ is the number of registers having value j .

Since the corresponding ML equation has the same shape as that for HLL, it can be solved in a numerically robust fashion using the secant method as described in [19]. This algorithm avoids the evaluation of expensive mathematical functions, but is still somewhat costly as the solution needs to be found iteratively. The ML estimate \hat{n}_{ML} can be further improved by correcting for the first-order bias [16]. Applying the correction factor as derived in Lemma 6 in Appendix A under the assumption of the simplified PMF (4) gives for ULL with $b = 2$ and $d = 2$

$$\hat{n} = \hat{n}_{\text{ML}} \left(1 + \frac{1}{m} \frac{3(\ln 2)\zeta(3, \frac{5}{4})}{2(\zeta(2, \frac{5}{4}))^2} \right)^{-1} \approx \hat{n}_{\text{ML}} \left(1 + \frac{0.48147}{m} \right)^{-1} \quad (10)$$

where ζ denotes again the Hurwitz zeta function.

The advantage of the ML method is its asymptotic efficiency as $m \rightarrow \infty$. The experimental results presented later in Section 4.1 show that the ML estimate really matches the theoretically predicted MVP (7). For HLL, estimators have been found that are easier to compute than the ML estimator while giving almost equal estimates over the whole value range [19]. This was our motivation for finding a simpler estimator for ULL.

2.5 Generalized Remaining Area Estimator

Recently, the generalized remaining area (GRA) estimator was proposed, which can be easily computed and is more efficient than existing estimators for probabilistic counting with stochastic averaging (PCSA) and HyperLogLog (HLL) [43]. Therefore, we investigated if this estimation approach is also suitable for our generalized data structure and in particular for ULL. The basic idea is to sum up $b^{-\tau k}$ with some constant $\tau > 0$ for all update values k that we know with certainty, based on the current register value $r = u2^d + \langle l_1 \dots l_d \rangle_2$, could not have occurred previously. The corresponding statistic for our generalized data structure can be expressed as $\sum_{k=u-d}^{u-1} (1 - l_{u-k}) b^{-\tau k} + \sum_{k=u+1}^{\infty} b^{-\tau k} = b^{-\tau u} \left(\frac{1}{b^{\tau} - 1} + \sum_{s=1}^d (1 - l_s) b^{\tau s} \right)$. The analysis of the first two moments of this statistic (cf. Lemmas 7 and 8 in Appendix A) under the assumption of the simplified PMF (4), together with the Delta method (see Lemma 12 in Appendix A) yields the distinct count estimator

$$\hat{n} = m^{1+\frac{1}{\tau}} \cdot \left(\sum_{i=0}^{m-1} g(r_i) \right)^{-\frac{1}{\tau}} \cdot \left(1 + \frac{1+\tau}{2} \frac{v}{m} \right)^{-1} \quad (11)$$

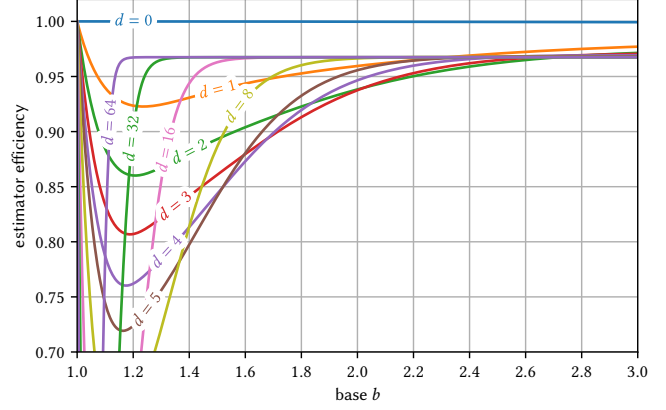


Figure 4: The asymptotic GRA estimator efficiency over the base b for $q = 6$ and various values of d .

where the individual register contributions are defined as

$$g(r) := \frac{(b-1+b^{-\tau})^\tau \ln b}{\Gamma(\tau)} b^{-\tau u} \left(\frac{1}{b^\tau - 1} + \sum_{s=1}^d (1 - l_s) b^{s\tau} \right) \quad (12)$$

with $r = u2^d + \langle l_1 \dots l_d \rangle_2$ and

$$v = \frac{1}{\tau^2} \left(\frac{\ln(b)\Gamma(2\tau)}{\Gamma(\tau)^2} \left(1 + \frac{2b^{-\tau d}}{b^\tau - 1} + \sum_{s=1}^d \frac{2b^{-\tau s}}{\left(1 + \frac{(b-1)b^{-s}}{b-1+b^{-d}} \right)^{2\tau}} \right) - 1 \right).$$

The last factor of the estimator (11) comes from applying the second-order Delta method [11] and corrects some bias similar to the last factor in (10).

As τ is a free parameter, it is ideally chosen to minimize the variance approximated by (see Lemma 12 in Appendix A)

$$\text{Var}(\hat{n}/n) \approx v/m + O(m^{-2}). \quad (13)$$

For ULL with $b = 2$ and $d = 2$, numerical minimization gives $v \approx 0.616990$ for $\tau \approx 0.755097$. In this case (12) can be written as

$$g(r) := 2^{-\tau \lfloor r/4 \rfloor} \eta_{r \bmod 4} \quad (14)$$

with coefficients

$$\eta_0 \approx 4.841356, \eta_1 \approx 2.539198, \eta_2 \approx 3.477312, \eta_3 \approx 1.175153.$$

The corresponding MVP is $8v = 4.935917$ which is slightly greater than the theoretical MVP (7) with a value of 4.631289. Hence, the efficiency of the GRA estimator is 93.8%.

Figure 4 shows the asymptotic GRA estimator efficiency as $m \rightarrow \infty$ relative to (7) over the base b for $q = 6$ and for various values of d . The GRA estimator is very efficient for $d = 0$ and therefore for HLL. It can be clearly seen that its efficiency is lower for other configurations with $d \geq 1$. Therefore, we investigated if we can find a more efficient estimator for ULL, that is as simple and cheap to evaluate as the GRA estimator.

2.6 New Estimator

Our idea is to further generalize the GRA estimator, by choosing not only τ but also the coefficients η_0, η_1, η_2 , and η_3 in (14) such that the variance is minimized. That is why we call the new estimator

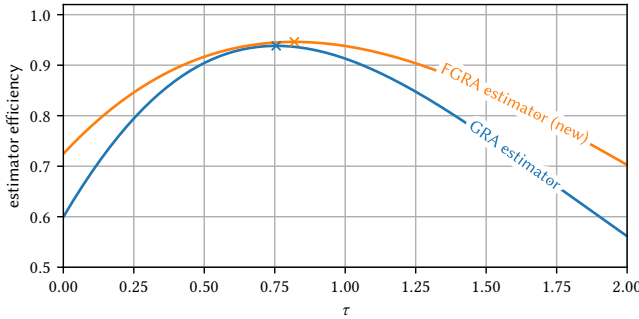


Figure 5: The efficiencies of the GRA estimator and our proposed FGRA estimator as a function of τ for $b = 2$ and $d = 2$. Crosses indicate optimal choices of τ .

further generalized remaining area (FGRA) estimator. As shown by Lemmas 9 to 12 in Appendix A the optimal values for $\eta_0, \eta_1, \eta_2, \eta_3$ for fixed τ are given by

$$\eta_j = \frac{\ln b}{\Gamma(\tau)} \frac{\omega_j(\tau)}{\omega_j(2\tau)} \left(\frac{\omega_0^2(\tau)}{\omega_0(2\tau)} + \frac{\omega_1^2(\tau)}{\omega_1(2\tau)} + \frac{\omega_2^2(\tau)}{\omega_2(2\tau)} + \frac{\omega_3^2(\tau)}{\omega_3(2\tau)} \right)^{-1} \quad (15)$$

with

$$\begin{aligned} \omega_0(\tau) &:= \frac{1}{(b^3-b+1)^\tau} - \frac{1}{b^{3\tau}}, \\ \omega_1(\tau) &:= \frac{1}{(b^2-b+1)^\tau} - \frac{1}{b^{2\tau}} - \frac{1}{(b^3-b+1)^\tau} + \frac{1}{b^{3\tau}}, \\ \omega_2(\tau) &:= \frac{1}{(b^3-b^2+1)^\tau} - \frac{1}{(b^3-b^2+b)^\tau} - \frac{1}{(b^3-b+1)^\tau} + \frac{1}{b^{3\tau}}, \\ \omega_3(\tau) &:= \frac{1}{(b^3-b+1)^\tau} - \frac{1}{(b^3-b^2+1)^\tau} + \frac{1}{(b^3-b^2+b)^\tau} - \frac{1}{b^{3\tau}} \\ &\quad - \frac{1}{(b^2-b+1)^\tau} + \frac{1}{b^{2\tau}} + 1 - \frac{1}{b^\tau}. \end{aligned}$$

The minimum variance is then given by (13) with

$$v = \frac{1}{\tau^2} \left(\frac{\Gamma(2\tau) \ln b}{(\Gamma(\tau))^2} \left(\frac{\omega_0^2(\tau)}{\omega_0(2\tau)} + \frac{\omega_1^2(\tau)}{\omega_1(2\tau)} + \frac{\omega_2^2(\tau)}{\omega_2(2\tau)} + \frac{\omega_3^2(\tau)}{\omega_3(2\tau)} \right)^{-1} - 1 \right).$$

Numerical minimization of this expression with regard to τ for the ULL case with $b = 2$ and $d = 2$ yields $\tau \approx 0.819491$ for which $v \approx 0.611893$ and the corresponding coefficients following (15) are

$$\eta_0 \approx 4.663136, \eta_1 \approx 2.137850, \eta_2 \approx 2.781145, \eta_3 \approx 0.982408. \quad (16)$$

The resulting MVP = $8v \approx 4.895145$ corresponds to an efficiency of 94.6%, which is a small improvement over the GRA estimator as shown in Figure 5.

An interesting but not optimal choice would be $\tau = 1$, since this would make exponentiations in (11) and (14) particularly cheap. The corresponding coefficients would be

$$\eta_0 \approx 6.037409, \eta_1 \approx 2.415940, \eta_2 \approx 3.364340, \eta_3 \approx 0.934924,$$

which result in $v \approx 0.617163$ and a MVP of $8v \approx 4.937304$, which corresponds to an efficiency of 93.8%. In contrast, the efficiency of the GRA estimator would already drop to 91.3% if $\tau = 1$ is chosen.

2.7 Small and Large Range Corrections

Both the GRA as well as our newly proposed FGRA estimator assume that register values are distributed according to (4) rather than (3). However, this is invalid for small or large register values corresponding to small and large distinct counts and will result in

incorrect estimates. Unfortunately, much previous work has not properly addressed estimation for these edge cases. For example, the estimation error of the original HLL estimator [22] exceeded the predicted asymptotic error significantly for certain distinct counts. To be useful in practice, the distinct count estimate should be within the same error bounds over the entire range. While the estimator for HLL was patched in the meantime [19, 26, 36, 40, 48], recent algorithms such as EHLL [31] or HyperLogLogLog [27] still suggest, like the original HLL algorithm [22], to switch between different estimators. However, the corresponding transitions are not seamless which results in discontinuous estimation errors [19]. In the following we present a technique, which generalizes ideas presented in our earlier works [19, 20], to compose estimators of kind (11) with specific estimators for small and large distinct counts such that the resulting estimator works seamlessly over the whole value range.

A register state $r = u^{2d} + \langle l_1 \dots l_d \rangle_2$ allows to draw conclusions about the occurrence of certain events A_k as introduced in Section 2.1. For example, if $u < w$, we know for sure that A_u has occurred while events A_k with $k > u$ have not occurred. Bit l_s indicates the occurrence of A_{u-s} as long as $u > s$. However, we know nothing about events A_k with $k < u - d$ or $k \leq 0$. We can derive the PMF $\tilde{\rho}_{\text{reg}}(\tilde{r}|r, n)$, conditioned on the secured information about event occurrences we know from r , for register values \tilde{r} following the simple model (4). For the case $d+1 \leq r < w2^d$, \tilde{r} and r will always be equal, which yields $\tilde{\rho}_{\text{reg}}(\tilde{r}|r, n) = [\tilde{r} = r]$ when using the Iverson bracket notation. A complete derivation of $\tilde{\rho}_{\text{reg}}(\tilde{r}|r, n)$ for ULL with $d = 2$ and $b = 2$ is given in Appendix A under Lemma 13.

Assuming that the distinct count is equal to the estimate \hat{n}_{alt} obtained by an alternative distinct count estimator, we define the corrected register contribution $g_{\text{corr}}(r)$, to be used in (11) as replacement for $g(r)$, as the expected register contribution of $g(\tilde{r})$ where \tilde{r} follows the conditional PMF $\tilde{\rho}_{\text{reg}}(\tilde{r}|r, n = \hat{n}_{\text{alt}})$

$$g_{\text{corr}}(r) = \sum_{\tilde{r}=-\infty}^{\infty} \tilde{\rho}_{\text{reg}}(\tilde{r}|r, n = \hat{n}_{\text{alt}}) g(\tilde{r}). \quad (17)$$

This approach leads to $g_{\text{corr}}(r) = g(r)$ for the case $(d+1)2^d \leq r < w2^d$. Hence, if all registers are in this intermediate range, the estimator (11) remains unchanged. This is expected as the PMF (3) and (4) are equivalent in this case. However, the corrected contributions $g_{\text{corr}}(r)$ of very small and very large register values will differ significantly from $g(r)$. For ULL with $d = 2$ and $b = 2$ where $g(r)$ follows (14), the corrected register contributions can be written as (see Lemma 14 in Appendix A)

$$g_{\text{corr}}(r) = \begin{cases} \sigma(\hat{z}_0) & r=0, \\ 2^{-\tau} \psi(\hat{z}_0) & r=4, \\ 4^{-\tau} (\hat{z}_0(\eta_0-\eta_1)+\eta_1) & r=8, \\ 4^{-\tau} (\hat{z}_0(\eta_2-\eta_3)+\eta_3) & r=10, \\ 2^{-\tau \lfloor r/4 \rfloor} \eta_r \bmod 4 & r \in [12, 4w), \\ \frac{\hat{z}_w(1+\sqrt{\hat{z}_w})\eta_0 + 2^{-\tau} \sqrt{\hat{z}_w}(\hat{z}_w(\eta_0-\eta_2)+\eta_2) + \varphi(\sqrt{\hat{z}_w})}{2^{\tau w}(1+\sqrt{\hat{z}_w})(1+\hat{z}_w)} & r=4w, \\ \frac{\hat{z}_w(1+\sqrt{\hat{z}_w})\eta_1 + 2^{-\tau} \sqrt{\hat{z}_w}(\hat{z}_w(\eta_0-\eta_2)+\eta_2) + \varphi(\sqrt{\hat{z}_w})}{2^{\tau w}(1+\sqrt{\hat{z}_w})(1+\hat{z}_w)} & r=4w+1, \\ \frac{\hat{z}_w(1+\sqrt{\hat{z}_w})\eta_2 + 2^{-\tau} \sqrt{\hat{z}_w}(\hat{z}_w(\eta_1-\eta_3)+\eta_3) + \varphi(\sqrt{\hat{z}_w})}{2^{\tau w}(1+\sqrt{\hat{z}_w})(1+\hat{z}_w)} & r=4w+2, \\ \frac{\hat{z}_w(1+\sqrt{\hat{z}_w})\eta_3 + 2^{-\tau} \sqrt{\hat{z}_w}(\hat{z}_w(\eta_1-\eta_3)+\eta_3) + \varphi(\sqrt{\hat{z}_w})}{2^{\tau w}(1+\sqrt{\hat{z}_w})(1+\hat{z}_w)} & r=4w+3. \end{cases} \quad (18)$$

Here the functions ψ , σ , and φ are defined as

$$\psi(z) := z(z(\eta_0 - \eta_1 - \eta_2 + \eta_3) + (\eta_2 - \eta_3) + (\eta_1 - \eta_3)) + \eta_3, \quad (19)$$

$$\sigma(z) := \frac{1}{z} \sum_{u=0}^{\infty} 2^{\tau u} (z^{2^u} - z^{2^{u+1}}) \psi(z^{2^{u+1}}), \quad (20)$$

$$\varphi(z) := \frac{4^{-\tau}}{1-z} \sum_{u=0}^{\infty} 2^{-\tau u} (z^{2^{-u-1}} - z^{2^{-u}}) \psi(z^{2^{-u}}) \quad (21)$$

$$= \frac{4^{-\tau}}{2 - 2^{-\tau}} \left(\frac{2\psi(z)\sqrt{z} + \sum_{u=1}^{\infty} \frac{z^{2^{-u-1}} (2\psi(z^{2^{-u}}) - (z^{2^{-u-1}} + z^{2^{-u}}) \psi(z^{2^{-u+1}}))}{2^{\tau u} \prod_{j=1}^{u+1} (1+z^{2^{-j}})}}{2^{\tau u} \prod_{j=1}^{u+1} (1+z^{2^{-j}})} \right).$$

Furthermore, \hat{z}_0 and \hat{z}_w are defined as $\hat{z}_0 := e^{-\frac{\hat{n}_{\text{alt}}}{m}}$ and $\hat{z}_w := e^{-\frac{\hat{n}_{\text{alt}}}{m^2 w}}$ and are therefore estimates of $z_0 = e^{-\frac{n}{m}}$ and $z_w = e^{-\frac{n}{m^2 w}}$, respectively. According to (18), \hat{z}_0 is only needed for register values from $\{0, 4, 8, 10\}$. Therefore, the estimator \hat{z}_0 must work well only for small distinct counts. Similarly, the estimator \hat{z}_w must work only for large distinct counts, when there are registers $\geq 4w$. Corresponding estimators for both cases are presented in the next sections.

The numerical evaluation of σ is very cheap, because only basic mathematical operations are involved and the infinite series converges quickly. The convergence is slowest for arguments \hat{z}_0 close to 1. The largest arguments smaller than 1 occur for distinct counts equal to 1, which implies $\hat{z}_0 \approx e^{-\frac{1}{m}}$. However, even in this extreme case, empirical analysis showed numerical convergence after the first $p + 7$ terms for any precision $p \in [3, 26]$ when using double-precision floating-point arithmetic. For not too small values of p , the estimation costs are dominated by the iteration over all $m = 2^p$ registers to sum up the individual register contributions.

When using 64-bit hash values, the maximum update value is given by $w = 65 - p$ (see Section 2.1). In this case, registers with values $\geq 4w$ are very unlikely in practice and the evaluation of φ is rarely needed. Nevertheless, it also can be computed efficiently with the second (more complex appearing) expression for φ , which converges numerically after at most 22 terms for any $p \in [3, 26]$.

2.8 Estimator for Small Distinct Counts

The original HLL algorithm [22] switches, in case of small distinct counts, to the estimator

$$\hat{n}_{\text{low}} = m \ln(m/c_0), \quad (22)$$

known from probabilistic linear counting [44]. $c_0 := |\{i | r_i = 0\}|$ denotes the number of registers that have never been updated. This estimator corresponds to the ML estimator, when considering just the number of registers with $r_i = 0$ and using $\Pr(r_i = 0) = z_0 = e^{-\frac{n}{m}}$ which follows from (3) for $b = 2$. For HLL, the combination of this estimator with (17) leads to the same correction terms as we have derived differently in [19]. The resulting so-called corrected raw (CR) estimator was shown to be nearly as efficient as the ML estimator.

This finding provides confidence that the same approach also works for ULL to correct the GRA/FGRA estimator. Even though (22) could be used again to estimate small distinct counts, we found a simple estimator that is able to exploit more information. We consider the four smallest possible register states $r_i \in \{0, 4, 8, 10\}$ with corresponding probabilities following (3) and apply the ML method to estimate $z_0 = e^{-\frac{n}{m}}$. As shown in Appendix A under Lemma 15 the resulting ML estimator can be written as

$$\hat{z}_0 = ((\sqrt{\beta^2 + 4\alpha\gamma} - \beta)/(2\alpha))^4. \quad (23)$$

Here α , β , γ are defined as

$$\alpha := m + 3(c_0 + c_4 + c_8 + c_{10}), \quad \beta := m - c_0 - c_4,$$

$$\gamma := 4c_0 + 2c_4 + 3c_8 + c_{10}$$

and $c_j := |\{i | r_i = j\}|$ is again the number of registers with value j .

2.9 Estimator for Large Distinct Counts

An estimator for large distinct counts can be found in a similar way through ML estimation when considering the largest 4 register states $r_i \in \{4w, 4w + 1, 4w + 2, 4w + 3\}$. As derived in Appendix A under Lemma 16 the ML estimator for $z_w = e^{-\frac{n}{m^2 w}}$ can be written as

$$\hat{z}_w = \sqrt{(\sqrt{\beta^2 + 4\alpha\gamma} - \beta)/(2\alpha)}. \quad (24)$$

Here α , β , γ are defined as

$$\alpha := m + 3(c_{4w} + c_{4w+1} + c_{4w+2} + c_{4w+3}),$$

$$\beta := c_{4w} + c_{4w+1} + 2c_{4w+2} + 2c_{4w+3},$$

$$\gamma := m + 2c_{4w} + c_{4w+2} - c_{4w+3}.$$

2.10 Martingale Estimator

If the data is not distributed and merging of sketches is not needed, the distinct count can be estimated in an online fashion by incremental updates, which is known as martingale or historic inverse probability (HIP) estimation [15, 39] and which even leads to smaller estimation errors. This estimation approach can also be used for ULL. It keeps track of the state change probability μ . Initially, $\mu = 1$ as the first update will certainly change the state. Whenever a register is changed, the probability of state changes for further elements decreases. The probability, that a new unseen element changes the ULL state is given by

$$h(r_0, \dots, r_{m-1}) = \sum_{i=0}^{m-1} h(r_i).$$

$h(r_i)$ returns the probability that register r_i is changed with the next new element. Obviously, we have $h(0) = \frac{1}{m}$ and $h(4w + 3) = 0$ for the smallest and largest possible states, respectively. In the general case we have (see Lemma 17 in Appendix A)

$$h(r) = \begin{cases} \frac{1}{m} & r = 0, \\ \frac{1}{2m} & r = 4, \\ \frac{3}{4m} & r = 8, \\ \frac{1}{4m} & r = 10, \\ \frac{7-2l_1-4l_2}{2^u m} & r = 4u + \langle l_1 l_2 \rangle_2, 3 \leq u < w, \\ \frac{3-l_1-2l_2}{2^{w-1} m} & r = 4w + \langle l_1 l_2 \rangle_2. \end{cases} \quad (25)$$

The martingale estimator is incremented with every state change by $\frac{1}{\mu}$ prior the update as demonstrated by Algorithm 2. μ itself can also be incrementally adjusted, such that the whole update takes constant time. The values of h can be stored in a lookup table. The martingale estimator is unbiased and optimal [34], but cannot be used if the data is distributed and mergeability is required. For our generalized data structure introduced in Section 2, the asymptotic MVP can be derived as (see Lemma 18 in Appendix A)

$$\text{MVP} \approx (q + d) \frac{1}{2} \ln(b) \left(1 + \frac{b^{-d}}{b-1}\right).$$

This expression is consistent with previous specific results reported for HLL [34] and EHLL [31] and is plotted in Figure 6 for $d = 6$ and

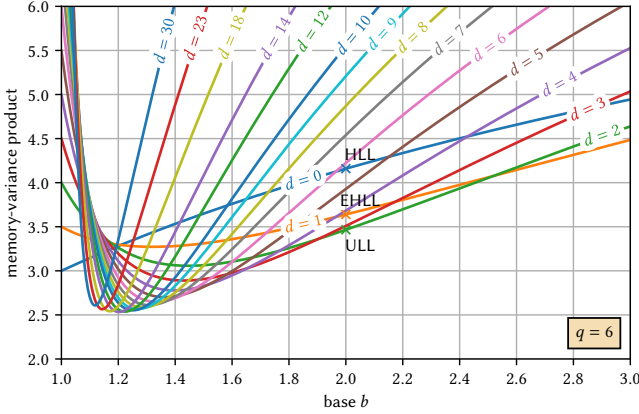


Figure 6: The MVP as a function of the base b for $q = 6$ and various values of d when using martingale estimation.

various values of b and d . For $b = 2$, the ULL configuration with $d = 2$ is even optimal. ULL achieves $\text{MVP} = 3.465736$ which is 17% less than for HLL with $\text{MVP} = 4.158883$.

3 PRACTICAL IMPLEMENTATION

As registers of ULL have $q + d = 8$ bits, they can be stored in a plain byte array. Algorithm 3 shows the update procedure for inserting an element. The actual input is the hash value of the element from which the register index i and an update value k are obtained. As for other probabilistic data structures it is essential to use a high-quality hash function such as WyHash [49] or Komihash [42] whose outputs are in practice indistinguishable from true random integers. If 64-bit hash values are used, the maximum update value is limited to $w = 65 - p$ leading to a maximum distinct count of roughly $n_{\max} \approx m2^{w-1} = 2^{64}$ which is more than sufficient for any realistic application.

Algorithm 3 updates the i -th register by first unpacking its value to a 64-bit value $x = \langle x_{63}x_{62} \dots x_1x_0 \rangle_2$ (see Algorithm 5) where bit x_{j+1} indicates the occurrence of update value j . After setting the corresponding bit for the new update value k , x is finally packed again into a register value (see Algorithm 4), preserving just the information about the maximum update value u and whether update values $u - 1$ and $u - 2$ have already occurred.

Although the update algorithm for HLL (cf. Algorithm 1) looks simpler, in practice the implementation complexity is similar if one also includes the bit twiddling required to pack 6-bit registers densely into a byte array. ULL insertions can be implemented entirely branch-free, as exemplified by the implementation in our Hash4j Java library (see <https://github.com/dynatrace-oss/hash4j>), which however uses the transformation $r \leftarrow r + 4p - 8$ for non-zero registers, so that the largest possible register state is always $(4w + 3) + 4p - 8 = 255$.

Algorithm 6 summarizes FGRA estimation including corrections for small and large distinct counts. If the registers are all in the range $[12, 4w]$, the algorithm just sums up the individual register contributions $g(r_i)$. The values of g can be pre-computed and stored in a lookup table for all possible register values. The final estimate is obtained by exponentiating the sum of all register contributions

Algorithm 2: Incrementally updates the martingale estimate $\hat{n}_{\text{martingale}}$ and the state change probability μ whenever a register is altered from r to r' ($r < r'$). Initially, $\hat{n}_{\text{martingale}} = 0$ and $\mu = 1$.

```

 $\hat{n}_{\text{martingale}} \leftarrow \hat{n}_{\text{martingale}} + \frac{1}{\mu}$  ▷ update estimate
 $\mu \leftarrow \mu - h(r) + h(r')$  ▷ update state change probability, see (25)

```

Algorithm 3: Inserts an element with 64-bit hash value $\langle h_{63}h_{62} \dots h_0 \rangle_2$ into an UltraLogLog with registers r_0, r_1, \dots, r_{m-1} , $m = 2^p$ ($p \geq 3$), and initial values $r_i = 0$.

```

 $i \leftarrow \langle h_{63}h_{62} \dots h_{64-p} \rangle_2$  ▷ extract register index
 $a \leftarrow \langle 0 \dots 0 h_{63-p}h_{62-p} \dots h_0 \rangle_2$  ▷ mask register index bits
 $k \leftarrow \text{nlz}(a) - p + 1$  ▷ update value  $k \in [1, 65 - p]$ 
 $x \leftarrow \text{unpack}(r_i)$  ▷ see Algorithm 5 for unpack
 $x \leftarrow x \text{ or } 2^{k+1}$  ▷ bitwise or-operation
 $r_i \leftarrow \text{pack}(x)$  ▷ see Algorithm 4 for pack

```

Algorithm 4: Packs a 64-bit value $x \geq 4$ into an 8-bit register. $x = \langle x_{63}x_{62} \dots x_1x_0 \rangle_2$ is interpreted as bitset where bit x_{k+1} indicates the occurrence of update value k .

```

function pack( $x$ )
   $u \leftarrow 62 - \text{nlz}(x)$  ▷ extract maximum update value
  return  $4u + \langle x_u x_{u-1} \dots x_0 \rangle_2$  ▷ return 8-bit register value, is always  $\geq 4$ 

```

Algorithm 5: Unpacks an 8-bit register $r = \langle q_7q_6 \dots q_0 \rangle_2$ into a 64-bit integer indicating the occurrence of update values if interpreted as bitset.

```

function unpack( $r$ )
  if  $r < 4$  then return 0 ▷ special case for initial state when  $r = 0$ 
   $u \leftarrow \langle q_7q_6 \dots q_2 \rangle_2$  ▷ get maximum update value, same as  $[r/4]$ 
  return  $\langle 0 \dots 0 q_1 q_0 0 \dots 0 \rangle_{62-u}$  ▷ return 64-bit value, is always  $\geq 4$ 

```

by $-\frac{1}{\tau}$ and multiplying by the precomputed factor λ_p . If there are any registers outside of $[12, 4w]$, the corresponding corrections need to be computed as previously described in Sections 2.7 to 2.9.

3.1 Merging and Downsizing

ULL sketches can be merged which is important if the data is distributed over space and/or time and partial results must be combined. The final result will only depend on the set of added elements and not on the insertion or merge order. It is even possible to merge ULL sketches with different precisions. For that, the sketch with higher precision must be reduced first to the lower precision of the other sketch.

Downsizing from precision p' to $p < p'$ is realized by merging the information of batches of $2^{p'-p}$ consecutive registers. The resulting register value depends not only on the individual register values, but also on the lower $p' - p$ bits of the register indices. Only the value of the first register of a batch, whose index has $p' - p$ trailing zeros, is relevant. All other registers need to be treated differently, as the $p' - p$ trailing index bits would have affected the calculation of the NLZ computation in Algorithm 3 when recorded with lower precision.

Algorithm 7 shows in detail how an ULL sketch with precision p' can be merged in-place into another one with precision $p \leq p'$. The algorithm simplifies a lot when the precisions are equal, because

Algorithm 6: Estimates the number of distinct elements from a given UltraLogLog with registers r_0, r_1, \dots, r_{m-1} and $m = 2^p$ ($p \geq 3$) using the FGRA estimator. The constants are defined as $w := 65 - p$, $\tau := 0.8194911850376387$, $v := 0.6118931496978426$, $\eta_0 := 4.663135749698441$, $\eta_1 := 2.137850286535751$, $\eta_2 := 2.7811447941454626$, $\eta_3 := 0.9824082439220764$, and $\lambda_p := m^{1+\frac{1}{\tau}}/(1 + \frac{1+\tau}{2} \frac{v}{m})$.

```

s ← 0                                ▶ used to sum up  $\sum_{i=0}^{m-1} g_{\text{corr}}(r_i)$ , see (18)
(c0, c4, c8, c10, c4w, c4w+1, c4w+2, c4w+3) ← (0, 0, 0, 0, 0, 0, 0)
for i ← 0 to m - 1 do
    if  $r_i < 12$  then
        if  $r_i = 0$  then  $c_0 \leftarrow c_0 + 1$ 
        if  $r_i = 4$  then  $c_4 \leftarrow c_4 + 1$ 
        if  $r_i = 8$  then  $c_8 \leftarrow c_8 + 1$ 
        if  $r_i = 10$  then  $c_{10} \leftarrow c_{10} + 1$ 
    else if  $r_i < 4w$  then
        s ← s + g(ri)                  ▶ see (14), g(ri) can be precomputed
    else
        if  $r_i = 4w$  then  $c_{4w} \leftarrow c_{4w} + 1$ 
        if  $r_i = 4w + 1$  then  $c_{4w+1} \leftarrow c_{4w+1} + 1$ 
        if  $r_i = 4w + 2$  then  $c_{4w+2} \leftarrow c_{4w+2} + 1$ 
        if  $r_i = 4w + 3$  then  $c_{4w+3} \leftarrow c_{4w+3} + 1$ 
    if  $c_0 + c_4 + c_8 + c_{10} > 0$  then
        α ← m + 3(c0 + c4 + c8 + c10)                                ▶ small range correction
        β ← m - c0 - c4
        γ ← 4c0 + 2c4 + 3c8 + c10
        z ← (( $\sqrt{\beta^2 + 4\alpha\gamma} - \beta$ )/(2α))4                                ▶ see (23)
        if  $c_0 > 0$  then s ← s + c0 · σ(z)                                ▶ for σ see (20)
        if  $c_4 > 0$  then s ← s + c4 · 2-τ · ψ(z)                                ▶ for ψ see (19)
        if  $c_8 > 0$  then s ← s + c8 · (4-τ · (z · (η0 - η1) + η1))
        if  $c_{10} > 0$  then s ← s + c10 · (4-τ · (z · (η2 - η3) + η3))
    if  $c_{4w} + c_{4w+1} + c_{4w+2} + c_{4w+3} > 0$  then
        α ← m + 3(c4w + c4w+1 + c4w+2 + c4w+3)                                ▶ large range correction
        β ← c4w + c4w+1 + 2c4w+2 + 2c4w+3
        γ ← m + 2c4w + c4w+2 - c4w+3
        z ←  $\sqrt{(\sqrt{\beta^2 + 4\alpha\gamma} - \beta)/(2\alpha)}$                                 ▶ see (24)
        z' ←  $\sqrt{z}$ 
        s' ← z · (1 + z') · (η0 · c4w + η1 · c4w+1 + η2 · c4w+2 + η3 · c4w+3)
        s' ← s' + 2-τ · z' · (z · (η0 - η2) + η2) · (c4w + c4w+1)
        s' ← s' + 2-τ · z' · (z · (η1 - η3) + η3) · (c4w+2 + c4w+3)
        s' ← s' + φ(z') · (c4w + c4w+1 + c4w+2 + c4w+3)                                ▶ for φ see (21)
        s ← s' / (2τw · (1 + z') · (1 + z))
    return  $\lambda_p \cdot s^{-1/\tau}$                                 ▶ return distinct count estimate, see (11)

```

$p' = p$ implies $2^{p'-p} = 1$ and consequently the inner loop can be skipped entirely. In this case, and also due to the byte-sized registers, the ULL merge operation is very well suited for single-instruction multiple-data (SIMD) processing.

Algorithm 7 can also be applied to just downsize a ULL sketch from precision p' to p , if the sketch is simply added to an empty ULL sketch with precision p and all registers equal to zero, $r_i = 0$. In this case the first unpack operation can be skipped as it would always return zero.

3.2 Compatibility to HyperLogLog

When using the same hash function for elements, ULL can be implemented in a way that is compatible with an existing HLL implementation meaning that an ULL sketch can be mapped to a HLL sketch of same precision by just dropping the last 2 register bits

Algorithm 7: Merges an UltraLogLog with registers $r'_0, r'_1, \dots, r'_{m'-1}$ and $m' = 2^{p'}$ into another UltraLogLog with registers r_0, r_1, \dots, r_{m-1} and $m = 2^p$ where $p \leq p'$. This algorithm also allows to downsize an existing UltraLogLog by merging it into an empty UltraLogLog ($r_i = 0$) with smaller precision parameter $p < p'$.

```

j ← 0
for i ← 0 to m - 1 do
    x ← unpack(ri) or (unpack(r'j) · 2p'-p)                                ▶ bitwise or-operation, see Algorithm 5 for unpack
    j ← j + 1
    for l ← 1 to 2p'-p - 1 do
        if r'j ≠ 0 then
            k ← nlz(l) + p' - p - 63          ▶ l is assumed to have 64 bits
            x ← x or 2k+1                                ▶ bitwise or-operation
        j ← j + 1
    if x ≠ 0 then ri ← pack(x)                                ▶ see Algorithm 4 for pack

```

corresponding to the transformation $r_i^{(\text{HLL})} \leftarrow \lfloor r_i^{(\text{ULL})} / 4 \rfloor$. This allows to migrate to ULL, even if there is historical data that was recorded using HLL and still needs to be combined with newer data. Our Hash4j library also contains a HLL implementation that is compatible with its ULL implementation.

4 EXPERIMENTS

Various experiments have been conducted to confirm the theoretical results and to demonstrate the practicality of ULL. Extensive empirical tests [41] have shown that the output of modern hash functions such as WyHash [49] or Komihash [42] can be considered like uniform random values. Otherwise, field-tested probabilistic data structures like HLL would not work. This fact allows us to simplify the experiments and perform them without real or artificially generated data. Insertion of a new element can be simulated by simply generating a 64-bit random value to be used directly as the hash value of the inserted element in Algorithm 3.

4.1 Estimation Error

To simulate the estimation error for a predefined distinct count value, the estimate is computed after updating the ULL sketch using Algorithm 3 with a corresponding number of random values and finally compared against the true distinct count. By repeating this process with many different random sequences, in our experiments 100000, the bias and the root-mean-square error (RMSE) can be empirically determined. However, this approach becomes computationally infeasible for distinct counts beyond 1 million and we need to switch to a different strategy. After the first million of insertions, for which a random value was generated each time, we just generate the waiting time (the number of increments) until a register is processed with a certain update value the next time. The probability that a register is updated with any possible value $k \in [1, 65 - p]$ is given by $1/(m2^{\min(k, 64-p)})$. Therefore, the number of distinct count increments until a register is updated with a specific value k the next time is geometrically distributed with corresponding success probability. In this way, we determine the next update time for each register and for each possible update value. Since the same update value can only modify a register once, we do not need to consider further updates which might occur with the same value

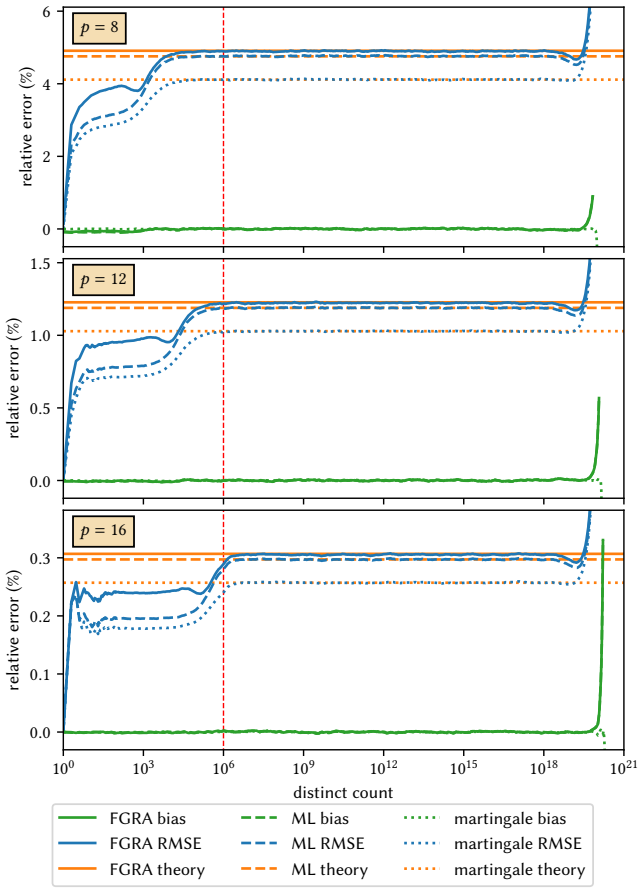


Figure 7: The relative bias and the RMSE for the FGRA, ML, and the martingale estimator for precisions $p \in \{8, 12, 16\}$ obtained from 100000 simulation runs. The theoretically predicted errors perfectly match the experimental results. Individual insertions were simulated up to a distinct count of 10^6 before switching to the fast simulation strategy.

for the same register. Knowing these $m \times (65 - p)$ distinct counts leading to possible state changes in advance, enables us to make large distinct count increments, resulting in a huge speedup. This eventually allowed us to simulate the estimation error for distinct counts up to values of 10^{21} and also to test the presented estimators over the entire operating range.

Figure 7 shows the empirically determined relative bias and RMSE as well as the theoretical RMSE given by $\sqrt{MVP}/(8m)$ for the FGRA, ML, and the martingale estimator for precisions $p \in \{8, 12, 16\}$. For intermediate distinct counts, for which the assumptions of our theoretical analysis hold, perfect agreement with theory is observed. For small distinct counts, the difference in efficiency between ML and FGRA is more significant, but not problematic as the estimation errors are still well below the predicted error. Interestingly, the estimation error also decreases slightly near the end of the operating range, which is as predicted on the order of $2^{64} \approx 1.9 \cdot 10^{19}$. The estimators are essentially unbiased. The

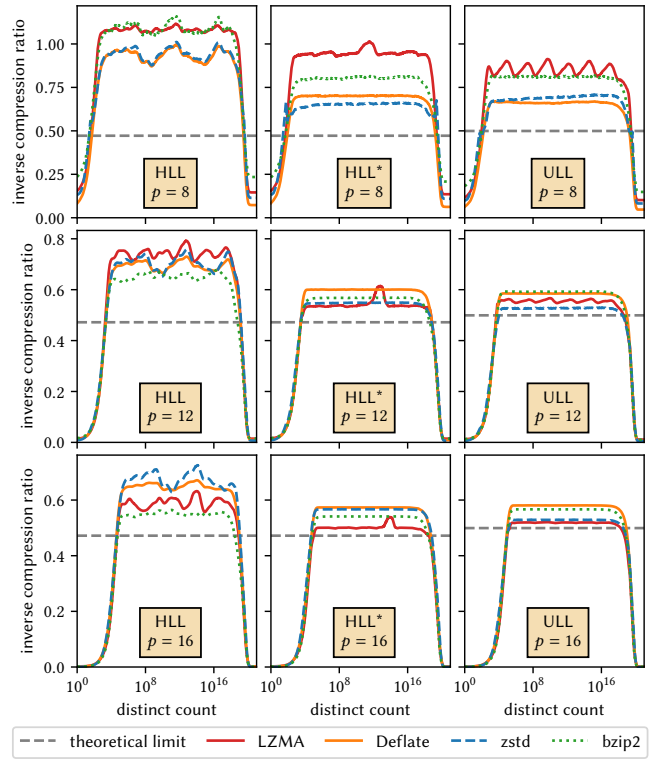


Figure 8: The average inverse compression ratio for HLL and ULL over the distinct count for various standard compression algorithms. For HLL*, the 6-bit registers are mapped to individual bytes before compression. The gray dashed line indicates the theoretical lower bound for intermediate distinct counts.

tiny bias which appears for small precisions for the ML and FGRA estimators can be ignored in practice as it is much smaller than the RMSE.

4.2 Compression

To analyze the compressibility of the state, we generated 100 random sketches for predefined distinct counts and applied various standard compression algorithms (LZMA, Deflate, zstd, and bzip2) from the Apache Compress Java library [1]. The corresponding average inverse compression ratios over the distinct count are shown in Figure 8 for HLL and ULL. The results indicate that the algorithms generally work better for ULL than HLL, since the compressed size is closer to the theoretical limit given by the Shannon entropy (8). Interestingly, the compression for HLL improves, if its 6-bit registers are first represented as individual bytes (cf. HLL* in Figure 8). Even though this leads to compression ratios that are sometimes better than for ULL, the latter is still more memory-efficient due to the significant lower MVP when uncompressed. The theoretical lower bound applies only to intermediate distinct counts under the validity of the simple model (4). The observed high compressibility at small and large distinct counts is due to the large number of initial and saturated registers, respectively. Therefore, many HLL

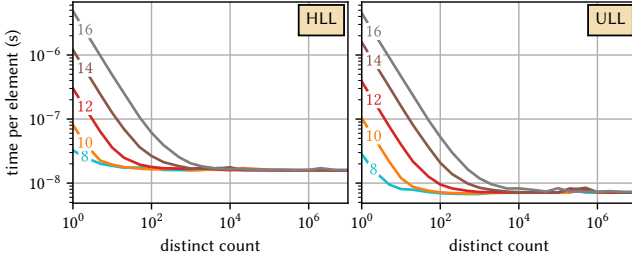


Figure 9: Average insertion time per element when initializing a HLL or ULL sketch with $p \in \{8, 10, 12, 14, 16\}$ and adding the given number of distinct elements.

implementations support a sparse mode that encodes only non-zero registers [26]. We expect that this and other lossless compression techniques developed for HLL [2, 27] can also be applied to ULL, but obviously at the cost of slower updates and memory reallocations.

4.3 Performance

Since low processing costs are also critical for practical use, we measured the average time for inserting a given number of distinct elements into HLL and ULL sketches configured with precisions $p \in \{8, 10, 12, 14, 16\}$. We used implementations of both from our Hash4j Java library (v0.11.0) and ran all experiments on a Dell Precision 5560 notebook with an Intel Core i9-11950HK processor clocked at 2.6 GHz. The measurements shown in Figure 9 also include sketch initialization as well as the generation of random numbers which were used instead of hash values as described before. The initialization costs dominate for small distinct counts, which are proportional to $m = 2^p$ due to the allocated register array. For large distinct counts the initialization costs can be neglected, and the average time per insertion converges to a value that is essentially independent of p . There, it becomes apparent that HLL insertions are significantly slower, mainly caused by the overhead of accessing the 6-bit registers packed in a byte array.

We also investigated the estimation costs for precisions $p \in [8, 16]$ and different distinct counts. We considered the ML estimator for both, the corrected raw (CR) estimator for HLL [19], and the new FGRA estimator for ULL. ML estimation is more expensive for ULL than for HLL for larger distinct counts. The CR and the FGRA estimator are most of the time significantly faster than their ML counterparts. The costs of the CR estimator are roughly constant, while the FGRA estimator peaks briefly before it falls back on the same level as the CR estimator for equal p . Our investigations showed that this peak is related to the more difficult branch prediction in Algorithm 6, when significant portions of registers have values from $\{0, 4, 8, 10\}$ and also values ≥ 12 .

In general, a fair comparison between HLL and ULL must take into account that an ULL sketch with same precision leads to smaller estimation errors. To have similar errors, we would have to set $\text{MVP}^{(\text{HLL})}/(6 \cdot 2^{p^{(\text{HLL})}}) = \text{MVP}^{(\text{ULL})}/(8 \cdot 2^{p^{(\text{ULL})}})$ leading to $p^{(\text{HLL})} \approx p^{(\text{ULL})} + 0.8$, which means that an ULL with $p = 8$ is rather compared to a HLL with $p = 9$ than $p = 8$. Thus, estimation from ULL using the FGRA estimator is often faster (except for the peaks) than from an HLL of equivalent precision using the CR estimator.

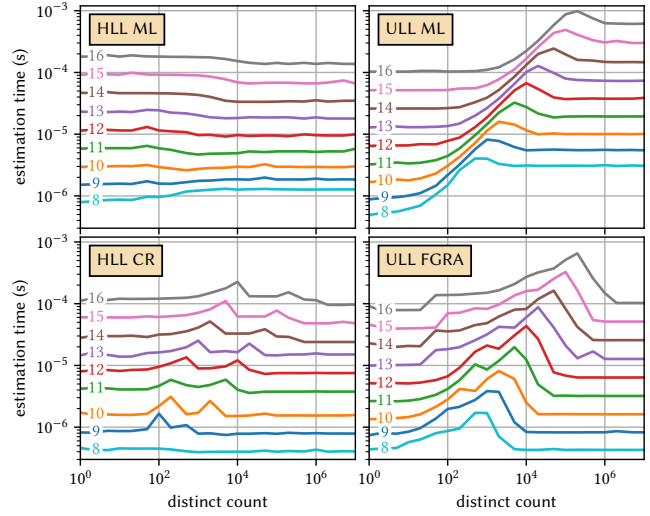


Figure 10: Average estimation time over the true distinct count for HLL and ULL for various precisions $p \in [8, 16]$.

5 CONCLUSION

We derived the ULL sketch as a special case of a generalized data structure unifying HLL, EHLL, and PCSA. The theoretically predicted space savings of 28%, 24%, and 17% over HLL when using the ML, FGRA, and martingale estimator, respectively, were perfectly matched by our experiments. The byte-sized registers lead to faster recording speed as well as better compressibility. Since ULL also has the same properties as HLL (constant-time insertions, idempotency, mergeability, reproducibility, reducibility), efficient and robust estimation with similar execution speed is possible, and even compatibility with HLL can be achieved, we believe that ULL has the potential to become the new standard algorithm for approximate distinct counting. Moreover, our theoretical results could trigger further research, as opportunities for even more space-efficient data structures have been identified.

REFERENCES

[1] [n.d.]. *Apache Commons Compress*. Retrieved August 23, 2023 from <https://commons.apache.org/proper/commons-compress/>

[2] [n.d.]. *Apache Data Sketches: A software library of stochastic streaming algorithms*. Retrieved August 23, 2023 from <https://dataskeches.apache.org/>

[3] [n.d.]. *Apache Data Sketches: Features Matrix for Distinct Count Sketches*. Retrieved August 23, 2023 from <https://dataskeches.apache.org/docs/DistinctCountFeaturesMatrix.html>

[4] [n.d.]. *Snowflake Documentation: Estimating the Number of Distinct Values*. Retrieved August 23, 2023 from <https://docs.snowflake.com/en/user-guide/querying-approximate-cardinality>

[5] N. Alon, Y. Matias, and M. Szegedy. 1999. The Space Complexity of Approximating the Frequency Moments. *J. Comput. System Sci.* 58, 1 (1999), 137–147. <https://doi.org/10.1006/jcss.1997.1545>

[6] D. N. Baker and B. Langmead. 2019. Dashing: fast and accurate genomic distances with HyperLogLog. *Genome Biology* 20, 265 (2019). <https://doi.org/10.1186/s13059-019-1875-0>

[7] R. B. Basav, G. Einziger, S. L. Feibish, J. Moranay, and D. Raz. 2018. Network-wide routing-oblivious heavy hitters. In *Proceedings of the 16th Symposium on Architectures for Networking and Communications Systems (ANCS)*. 66–73. <https://doi.org/10.1145/3230718.3230729>

[8] P. Boldi, M. Rosa, and S. Vigna. 2011. HyperANF: Approximating the neighbourhood function of very large graphs on a budget. In *Proceedings of the 20th International Conference on World Wide Web (WWW)*. 625–634. <https://doi.org/10.1145/1963405.1963493>

[9] F. P. Breitwieser, D. N. Baker, and S. L. Salzberg. 2018. KrakenUniq: confident and fast metagenomics classification using unique k-mer counts. *Genome biology* 19, 1 (2018), 1–10. <https://doi.org/10.1186/s13059-018-1568-0>

[10] V. Bruschi, P. Reviriego, S. Pontarelli, D. Ting, and G. Bianchi. 2021. More Accurate Streaming Cardinality Estimation With Vectorized Counters. *IEEE Networking Letters* 3, 2 (2021), 75–79. <https://doi.org/10.1109/LNET.2021.3076048>

[11] G. Casella and R. L. Berger. 2002. *Statistical Inference* (2nd ed.). Duxbury, Pacific Grove, CA.

[12] Y. Chabchoub, R. Chiky, and B. Dogan. 2014. How can sliding HyperLogLog and EWMA detect port scan attacks in IP traffic? *EURASIP Journal on Information Security* 2014, 5 (2014). <https://doi.org/10.1186/1687-417X-2014-5>

[13] A. Chen, J. Cao, L. Shepp, and T. Nguyen. 2011. Distinct Counting With a Self-Learning Bitmap. *J. Amer. Statist. Assoc.* 106, 495 (2011), 879–890. <https://doi.org/10.1198/jasa.2011.ap10217>

[14] V. Clemens, L.-C. Schulz, M. Gartner, and D. Hausheer. 2023. DDoS Detection in P4 Using HYPERLOGLOG and COUNTMIN Sketches. In *Network Operations and Management Symposium (NOMS)*. 1–6. <https://doi.org/10.1109/NOMS56928.2023.10154315>

[15] E. Cohen. 2015. All-Distances Sketches, Revisited: HIP Estimators for Massive Graphs Analysis. *IEEE Transactions on Knowledge and Data Engineering* 27, 9 (2015), 2320–2334. <https://doi.org/10.1109/TKDE.2015.2411606>

[16] D. R. Cox and E. J. Snell. 1968. A General Definition of Residuals. *Journal of the Royal Statistical Society. Series B (Methodological)* 30, 2 (1968), 248–275. <http://www.jstor.org/stable/2984505>

[17] M. Durand. 2004. *Combinatoire analytique et algorithmique des ensembles de données*. Ph.D. Dissertation. École Polytechnique, Palaiseau, France. <https://pastel.hal.science/pastel-00000810>

[18] R. A. L. Elworth, Q. Wang, P. K. Kota, C. J. Barberan, B. Coleman, A. Balaji, G. Gupta, R. G. Baraniuk, A. Shrivastava, and T. J. Treangen. 2020. To Petabytes and beyond: recent advances in probabilistic and signal processing algorithms and their application to metagenomics. *Nucleic Acids Research* 48, 10 (2020), 5217–5234. <https://doi.org/10.1093/nar/gkaa265>

[19] O. Ertl. 2017. New cardinality estimation algorithms for HyperLogLog sketches. (2017). [arXiv:1702.01284 \[cs.DS\]](https://arxiv.org/abs/1702.01284)

[20] O. Ertl. 2021. SetSketch: Filling the Gap between MinHash and HyperLogLog (extended version). (2021). [arXiv:2101.00314 \[cs.DS\]](https://arxiv.org/abs/2101.00314)

[21] O. Ertl. 2023. UltraLogLog: A Practical and More Space-Efficient Alternative to HyperLogLog for Approximate Distinct Counting (extended version). (2023). [arXiv:2308.16862 \[cs.DS\]](https://arxiv.org/abs/2308.16862)

[22] P. Flajolet, É. Fusy, O. Gandouet, and F. Meunier. 2007. HyperLogLog: the analysis of a near-optimal cardinality estimation algorithm. In *Proceedings of the International Conference on the Analysis of Algorithms (AofA)*. 127–146. <https://doi.org/10.46298/dmtcs.3545>

[23] P. Flajolet and G. N. Martin. 1985. Probabilistic counting algorithms for data base applications. *Journal of computer and system sciences* 31, 2 (1985), 182–209. [https://doi.org/10.1016/0022-0000\(85\)90041-8](https://doi.org/10.1016/0022-0000(85)90041-8)

[24] M. J. Freitag and T. Neumann. 2019. Every Row Counts: Combining Sketches and Sampling for Accurate Group-By Result Estimates. In *Proceedings of the 9th Conference on Innovative Data Systems Research (CIDR)*.

[25] A. Helmi, J. Lumbroso, C. Martínez, and A. Viola. 2012. Data Streams as Random Permutations: the Distinct Element Problem. In *Proceedings of the 23rd International Meeting on Probabilistic, Combinatorial, and Asymptotic Methods in the Analysis of Algorithms (AofA)*. 323–338. <https://doi.org/10.46298/dmtcs.3002>

[26] S. Heule, M. Nunkesser, and A. Hall. 2013. HyperLogLog in Practice: Algorithmic Engineering of a State of the Art Cardinality Estimation Algorithm. In *Proceedings of the 16th International Conference on Extending Database Technology (EDBT)*. 683–692. <https://doi.org/10.1145/2452376.2452456>

[27] M. Karppa and R. Pagh. 2022. HyperLogLogLog: Cardinality Estimation With One Log More. In *Proceedings of the 28th ACM SIGKDD Conference on Knowledge Discovery and Data Mining (KDD)*. 753–761. <https://doi.org/10.1145/3534678.3539246>

[28] K. J. Lang. 2017. Back to the Future: an Even More Nearly Optimal Cardinality Estimation Algorithm. (2017). [arXiv:1708.06839 \[cs.DS\]](https://arxiv.org/abs/1708.06839)

[29] J. Lu, H. Chen, J. Zhang, T. Hu, P. Sun, and Z. Zhang. 2023. Virtual self-adaptive bitmap for online cardinality estimation. *Information Systems* 114, 102160 (2023). <https://doi.org/10.1016/j.is.2022.102160>

[30] C. Marçais, B. Solomon, R. Patro, and C. Kingsford. 2019. Sketching and Sublinear Data Structures in Genomics. *Annual Review of Biomedical Data Science* 2, 1 (2019), 93–118. <https://doi.org/10.1146/annurev-biodatasci-072018-021156>

[31] T. Ohayon. 2021. ExtendedHyperLogLog: Analysis of a new Cardinality Estimator. (2021). [arXiv:2106.06525 \[cs.DS\]](https://arxiv.org/abs/2106.06525)

[32] C. Pavlopoulou, M. J. Carey, and V. J. Tsotras. 2022. Revisiting Runtime Dynamic Optimization for Join Queries in Big Data Management Systems. In *Proceedings of the 25th International Conference on Extending Database Technology (EDBT)*. <https://doi.org/10.5441/002/edbt.2022.01>

[33] S. Pettie and D. Wang. 2021. Information Theoretic Limits of Cardinality Estimation: Fisher Meets Shannon. In *Proceedings of the 53rd Annual ACM SIGACT Symposium on Theory of Computing (STOC)*. 556–569. <https://doi.org/10.1145/3406325.3451032>

[34] S. Pettie, D. Wang, and L. Yin. 2021. Non-Mergeable Sketching for Cardinality Estimation. In *48th International Colloquium on Automata, Languages, and Programming (ICALP)*, Vol. 198. 104:1–104:20. <https://doi.org/10.4230/LIPIcs.ICALP.2021.104>

[35] B. W. Priest, R. Pearce, and G. Sanders. 2018. Estimating Edge-Local Triangle Count Heavy Hitters in Edge-Linear Time and Almost-Vertex-Linear Space. In *Proceedings of the IEEE High Performance Extreme Computing Conference (HPEC)*. <https://doi.org/10.1109/HPEC.2018.8547721>

[36] J. Qin, D. Kim, and Y. Tung. 2016. LogLog-Beta and More: A New Algorithm for Cardinality Estimation Based on LogLog Counting. (2016). [arXiv:1612.02284 \[cs.DS\]](https://arxiv.org/abs/1612.02284)

[37] B. Scheuermann and M. Mauve. 2007. Near-optimal compression of probabilistic counting sketches for networking applications. In *Proceedings of the 4th ACM International Workshop on Foundations of Mobile Computing (FOMC)*.

[38] R. Sedgewick. 2022. HyperBit: A Memory-Efficient Alternative to HyperLogLog. (2022). <https://www.birs.ca/workshops/2022/22w5004/files/BobSedgewick/HyperBit.pdf> Analytic and Probabilistic Combinatorics Workshop at the Banff International Research Station (BIRS) for Mathematical Innovation and Discovery.

[39] D. Ting. 2014. Streamed Approximate Counting of Distinct Elements: Beating Optimal Batch Methods. In *Proceedings of the 20th ACM SIGKDD International Conference on Knowledge Discovery and Data Mining (KDD)*. 442–451. <https://doi.org/10.1145/2623330.2623669>

[40] D. Ting. 2019. Approximate distinct counts for billions of datasets. In *Proceedings of the International Conference on Management of Data (SIGMOD)*. 69–86. <https://doi.org/10.1145/3299869.3319897>

[41] R. Urban. [n.d.]. *SMhasher: Hash function quality and speed tests*. Retrieved August 23, 2023 from <https://github.com/rurban/smhasher>

[42] A. Vaneev. [n.d.]. *Komihash*. Retrieved August 23, 2023 from <https://github.com/avaneev/komihash/tree/b27fd61808f92a1fae617b4ecd0981cc69d31a0>

[43] D. Wang and S. Pettie. 2023. Better Cardinality Estimators for HyperLogLog, PCSA, and Beyond. In *Proceedings of the 42nd ACM Symposium on Principles of Database Systems (PODS)*. 317–327. <https://doi.org/10.1145/3584372.3588680>

[44] K.-Y. Whang, B. T. Vander-Zanden, and H. M. Taylor. 1990. A Linear-Time Probabilistic Counting Algorithm for Database Applications. *ACM Transactions on Database Systems* 15, 2 (1990), 208–229. <https://doi.org/10.1145/78922.78925>

[45] J. Wires, S. Ingram, Z. Drudi, N. J. A. Harvey, and A. Warfield. 2014. Characterizing storage workloads with counter stacks. In *11th USENIX Symposium on Operating Systems Design and Implementation (OSDI)*. 335–349. <https://www.usenix.org/conference/osdi14/technical-sessions/presentation/wires>

[46] Q. Xiao, S. Chen, Y. Zhou, M. Chen, J. Luo, T. Li, and Y. Ling. 2017. Cardinality estimation for elephant flows: A compact solution based on virtual register sharing. *IEEE/ACM Transactions on Networking* 25, 6 (2017), 3738–3752. <https://doi.org/10.1109/TNET.2017.2753842>

[47] Q. Xiao, Y. Zhou, and S. Chen. 2017. Better with fewer bits: Improving the performance of cardinality estimation of large data streams. In *IEEE Conference on Computer Communications (IEEE INFOCOM)*. 1–9. <https://doi.org/10.1109/INFOCOM.2017.8057088>

[48] Y. Zhao, S. Guo, and Y. Yang. 2016. Hermes: An Optimization of HyperLogLog Counting in real-time data processing. In *Proceedings of the International Joint Conference on Neural Networks (IJCNN)*. 1890–1895. <https://doi.org/10.1109/IJCNN.2016.7727507>

[49] W. Yi. [n.d.]. *Wyhash*. Retrieved August 23, 2023 from <https://github.com/wangyi-fudan/wyhash>

A PROOFS

LEMMA 1. If $z_u := e^{-\frac{n(b-1)}{mb^u}}$ with $n, m > 0$ and $b > 1$ the following identities hold:

$$\begin{aligned} z_u^b &= z_{u-1}, \\ \ln z_u &= -\frac{n}{m} \frac{b-1}{b^u}, \\ \frac{\partial}{\partial n} z_u &= \frac{1}{n} z_u \ln z_u, \\ \frac{\partial}{\partial n} \ln z_u &= \frac{1}{n} \ln z_u, \\ \frac{\partial^2}{\partial n^2} \ln z_u &= 0, \\ \frac{\partial}{\partial n} \ln(1-z_u) &= -\frac{1}{n} \frac{z_u \ln z_u}{1-z_u}, \\ \frac{\partial^2}{\partial n^2} \ln(1-z_u) &= -\frac{1}{n^2} \frac{z_u \ln^2 z_u}{(1-z_u)^2}, \\ \frac{\partial^3}{\partial n^3} \ln(1-z_u) &= -\frac{1}{n^3} \frac{z_u (1+z_u) \ln^3 z_u}{(1-z_u)^3}. \end{aligned}$$

PROOF. The proof is straightforward using basic calculus. \square

LEMMA 2. If $z_u := e^{-\frac{n(b-1)}{mb^u}}$ ($n, m > 0$ and $b > 1$) and f is a smooth function on $(0, 1)$ with $f(0+) = 0$ and $f(1-) = 0$, the series $\sum_{u=-\infty}^{\infty} f(z_u)$ is a periodic function of $\log_b(n)$ with period 1. Furthermore, if the relative amplitude can be neglected, the following approximation can be used

$$\sum_{u=-\infty}^{\infty} f(z_u) \approx \frac{1}{\ln b} \int_0^{\infty} \frac{f(e^{-y})}{y} dy = -\frac{1}{\ln b} \int_0^1 \frac{f(z)}{z \ln z} dz.$$

PROOF. The periodicity of the series is shown by

$$\begin{aligned} \sum_{u=-\infty}^{\infty} f(z_u) &= \sum_{u=-\infty}^{\infty} f\left(e^{-\frac{n(b-1)}{mb^u}}\right) \\ &= \sum_{u=-\infty}^{\infty} f\left(e^{-\frac{b-1}{mb^{u-\log_b(n)}}}\right) = \sum_{u=-\infty}^{\infty} f\left(e^{-\frac{b-1}{mb^{u-(1+\log_b(n))}}}\right). \end{aligned}$$

If its relative amplitude can be neglected, we can approximate

$$\begin{aligned} \sum_{u=-\infty}^{\infty} f(z_u) &= \sum_{u=-\infty}^{\infty} f\left(e^{-\frac{b-1}{mb^{u-\log_b(n)}}}\right) \\ &\approx \int_0^1 \sum_{u=-\infty}^{\infty} f\left(e^{-\frac{b-1}{mb^{u-x}}}\right) dx = \int_{-\infty}^{\infty} f\left(e^{-\frac{(b-1)b^x}{m}}\right) dx \\ &= \frac{1}{\ln b} \int_0^{\infty} \frac{f(e^{-y})}{y} dy = -\frac{1}{\ln b} \int_0^1 \frac{f(z)}{z \ln z} dz. \end{aligned}$$

\square

LEMMA 3. For the PMF given in (4) the following identity holds:

$$\begin{aligned} \sum_{l_1, \dots, l_d \in \{0,1\}} \tilde{\rho}_{\text{reg}}(u2^d + \langle l_1 \dots l_d \rangle_2 | n) \prod_{s=1}^d l_s^{\alpha_s} (1-l_s)^{\beta_s} \\ = z_u^{\frac{1}{b-1}} (1-z_u) \prod_{s=1}^d (1-z_{u-s})^{\alpha_s} z_{u-s}^{\beta_s} \end{aligned}$$

where $\alpha_s, \beta_s \in \{0, 1\}$, $\alpha_s + \beta_s \leq 1$, and 0^0 is defined as 1. As special cases, we have

$$\begin{aligned} \sum_{l_1, \dots, l_d \in \{0,1\}} \tilde{\rho}_{\text{reg}}(u2^d + \langle l_1 \dots l_d \rangle_2 | n) l_s &= z_u^{\frac{1}{b-1}} (1-z_u) (1-z_{u-s}), \\ \sum_{l_1, \dots, l_d \in \{0,1\}} \tilde{\rho}_{\text{reg}}(u2^d + \langle l_1 \dots l_d \rangle_2 | n) (1-l_s) &= z_u^{\frac{1}{b-1}} (1-z_u) z_{u-s}, \\ \sum_{l_1, \dots, l_d \in \{0,1\}} \tilde{\rho}_{\text{reg}}(u2^d + \langle l_1 \dots l_d \rangle_2 | n) &= z_u^{\frac{1}{b-1}} (1-z_u). \end{aligned}$$

PROOF.

$$\begin{aligned} &\sum_{l_1, \dots, l_d \in \{0,1\}} \tilde{\rho}_{\text{reg}}(u2^d + \langle l_1 \dots l_d \rangle_2 | n) \prod_{s=1}^d l_s^{\alpha_s} (1-l_s)^{\beta_s} \\ &= \sum_{l_1, \dots, l_d \in \{0,1\}} z_u^{\frac{1}{b-1}} (1-z_u) \prod_{j=1}^d z_{u-j}^{1-l_j} (1-z_{u-j})^{l_j} \prod_{s=1}^d l_s^{\alpha_s} (1-l_s)^{\beta_s} \\ &= \sum_{l_1, \dots, l_d \in \{0,1\}} z_u^{\frac{1}{b-1}} (1-z_u) \prod_{s=1}^d z_{u-s}^{1-l_s} (1-z_{u-s})^{l_s} l_s^{\alpha_s} (1-l_s)^{\beta_s} \\ &= z_u^{\frac{1}{b-1}} (1-z_u) \prod_{s=1}^d \sum_{l_s \in \{0,1\}} z_{u-s}^{1-l_s} (1-z_{u-s})^{l_s} l_s^{\alpha_s} (1-l_s)^{\beta_s} \\ &= z_u^{\frac{1}{b-1}} (1-z_u) \prod_{s=1}^d z_{u-s} 0^{\alpha_s} + (1-z_{u-s}) 0^{\beta_s} \\ &= z_u^{\frac{1}{b-1}} (1-z_u) \prod_{s=1}^d (1-z_{u-s})^{\alpha_s} z_{u-s}^{\beta_s}. \end{aligned}$$

The last equality can be verified by considering all possible cases $(\alpha_s, \beta_s) \in \{(0,0), (1,0), (0,1)\}$. \square

LEMMA 4. The Fisher information \mathcal{I} of random variables r_0, r_1, \dots, r_{m-1} that are distributed according to (4), can be approximated with Lemma 2 by

$$\mathcal{I} = \mathbb{E}\left(-\frac{\partial^2 \ln \mathcal{L}}{\partial n^2}\right) \approx \frac{m}{n^2} \frac{1}{\ln b} \zeta\left(2, 1 + \frac{b-d}{b-1}\right).$$

ζ denotes the Hurwitz zeta function $\zeta(x, y) := \sum_{u=0}^{\infty} (u+y)^{-x} = \frac{1}{\Gamma(x)} \int_0^{\infty} \frac{z^{x-1} e^{-yz}}{1-e^{-z}} dz$.

PROOF. Since the registers are independent under the Poisson approximation, it is sufficient to consider a single register and multiply the result by m

$$\begin{aligned} \mathcal{I} &= \mathbb{E}\left(-\frac{\partial^2 \ln \mathcal{L}}{\partial n^2}\right) = -m \sum_{r=-\infty}^{\infty} \tilde{\rho}_{\text{reg}}(r | n) \frac{\partial^2 \ln \tilde{\rho}_{\text{reg}}(r | n)}{\partial n^2} \\ &= \frac{m}{n^2} \sum_{u=-\infty}^{\infty} \sum_{l_1, \dots, l_d \in \{0,1\}} \tilde{\rho}_{\text{reg}}(u2^d + \langle l_1 \dots l_d \rangle_2 | n) \cdot \\ &\quad \cdot \left(\frac{z_u \ln^2 z_u}{(1-z_u)^2} + \sum_{j=1}^d l_j \frac{z_{u-j} \ln^2 z_{u-j}}{(1-z_{u-j})^2} \right). \end{aligned}$$

Here we used (4) and Lemma 1 for the second-order derivatives. With the help of Lemma 3 we can write

$$\begin{aligned} I &= \frac{m}{n^2} \sum_{u=-\infty}^{\infty} z_u^{\frac{1}{b-1}} (1-z_u) \left(\frac{z_u \ln^2 z_u}{(1-z_u)^2} + \sum_{j=1}^d \frac{z_{u-j} \ln^2 z_{u-j}}{1-z_{u-j}} \right) \\ &= \frac{m}{n^2} \sum_{u=-\infty}^{\infty} \left(\frac{z_u^{\frac{b}{b-1}} \ln^2 z_u}{1-z_u} + \sum_{j=1}^d \frac{z_u^{\frac{b}{b-1}} (1-z_u) z_{u-j} \ln^2 z_{u-j}}{1-z_{u-j}} \right) \\ &= \frac{m}{n^2} \sum_{u=-\infty}^{\infty} \left(\frac{z_u^{\frac{1}{b-1}}}{1-z_u} + \sum_{j=1}^d \frac{z_{u+j}^{\frac{1}{b-1}} - z_{u+j-1}^{\frac{1}{b-1}}}{1-z_u} \right) z_u \ln^2 z_u \\ &= \frac{m}{n^2} \sum_{u=-\infty}^{\infty} z_{u+d}^{\frac{1}{b-1}} \frac{z_u \ln^2 z_u}{1-z_u} = \frac{m}{n^2} \sum_{u=-\infty}^{\infty} z_u^{\frac{1+b-d}{b-1}} \ln^2 z_u. \end{aligned}$$

Using Lemma 2 with $f(x) = \frac{x^{1+\frac{b-d}{b-1}} \ln^2 x}{1-x}$ finally gives

$$I \approx \frac{m}{n^2 \ln b} \int_0^\infty \frac{e^{-y(1+\frac{b-d}{b-1})} y}{1-e^{-y}} dy = \frac{m}{n^2 \ln b} \zeta \left(2, 1 + \frac{b-d}{b-1} \right). \quad \square$$

LEMMA 5. The Shannon entropy \mathcal{H} of random variables r_0, r_1, \dots, r_{m-1} that are distributed according to (4) can be approximated with Lemma 2 by

$$\mathcal{H} \approx \frac{m}{(\ln 2)(\ln b)} \left(\left(1 + \frac{b-d}{b-1} \right)^{-1} + \int_0^1 z^{\frac{b-d}{b-1}} \frac{(1-z) \ln(1-z)}{z \ln(z)} dz \right).$$

PROOF. Since the registers are independent under the Poisson approximation, we can write the expectation of $\ln \mathcal{L}$ as

$$\begin{aligned} \mathbb{E}(\ln \mathcal{L}) &= m \sum_{r=-\infty}^{\infty} \tilde{\rho}_{\text{reg}}(r|n) \ln \tilde{\rho}_{\text{reg}}(r|n) \\ &= m \sum_{u=-\infty}^{\infty} \sum_{l_1, \dots, l_d \in \{0,1\}} \tilde{\rho}_{\text{reg}}(u2^d + \langle l_1 \dots l_d \rangle_2 | n) \cdot \\ &\quad \cdot \ln \left(z_u^{\frac{1}{b-1}} (1-z_u) \prod_{j=1}^d z_{u-j}^{1-l_j} (1-z_{u-j})^{l_j} \right) \\ &= m \sum_{u=-\infty}^{\infty} \sum_{l_1, \dots, l_d \in \{0,1\}} \tilde{\rho}_{\text{reg}}(u2^d + \langle l_1 \dots l_d \rangle_2 | n) \cdot \\ &\quad \cdot \left(\frac{\ln(z_u)}{b-1} + \ln(1-z_u) + \sum_{j=1}^d (1-l_j) \ln(z_{u-j}) + l_j \ln(1-z_{u-j}) \right). \end{aligned}$$

Here we used (4). Lemma 3 allows to write

$$\begin{aligned} \mathbb{E}(\ln \mathcal{L}) &= m \sum_{u=-\infty}^{\infty} z_u^{\frac{1}{b-1}} (1-z_u) \left(\frac{\ln(z_u)}{b-1} + \ln(1-z_u) \right) \\ &\quad + m \sum_{u=-\infty}^{\infty} \sum_{j=1}^d z_u^{\frac{1}{b-1}} (1-z_u) \left(z_{u-j} \ln(z_{u-j}) + (1-z_{u-j}) \ln(1-z_{u-j}) \right) \\ &= m \sum_{u=-\infty}^{\infty} z_u^{\frac{1}{b-1}} (1-z_u) \left(\frac{\ln(z_u)}{b-1} + \ln(1-z_u) \right) \end{aligned}$$

$$\begin{aligned} &+ m \sum_{u=-\infty}^{\infty} \sum_{j=1}^d (z_{u+j}^{\frac{1}{b-1}} - z_{u+j-1}^{\frac{1}{b-1}}) \left(z_u \ln(z_u) + (1-z_u) \ln(1-z_u) \right) \\ &= m \sum_{u=-\infty}^{\infty} z_u^{\frac{1}{b-1}} (1-z_u) \left(\frac{\ln(z_u)}{b-1} + \ln(1-z_u) \right) \\ &\quad + m \sum_{u=-\infty}^{\infty} (z_{u+d}^{\frac{1}{b-1}} - z_u^{\frac{1}{b-1}}) (z_u \ln(z_u) + (1-z_u) \ln(1-z_u)) \\ &= m \sum_{u=-\infty}^{\infty} z_u^{\frac{1}{b-1}} (1-z_u) \frac{\ln(z_u)}{b-1} - z_u^{\frac{1}{b-1}} z_u \ln(z_u) \\ &\quad + m \sum_{u=-\infty}^{\infty} z_{u+d}^{\frac{1}{b-1}} (z_u \ln(z_u) + (1-z_u) \ln(1-z_u)) \\ &= m \sum_{u=-\infty}^{\infty} z_u^{\frac{1}{b-1}} (1-z_u) \frac{\ln(z_u)}{b-1} - z_u^{\frac{1}{b-1}} z_u \ln(z_u) \\ &\quad + m \sum_{u=-\infty}^{\infty} z_u^{\frac{b-d}{b-1}} (z_u \ln(z_u) + (1-z_u) \ln(1-z_u)) \\ &= m \sum_{u=-\infty}^{\infty} \frac{z_u^{\frac{1}{b-1}} \ln(z_u) (1-z_u b)}{b-1} \\ &\quad + m \sum_{u=-\infty}^{\infty} z_u^{\frac{b-d}{b-1}} (z_u \ln(z_u) + (1-z_u) \ln(1-z_u)). \end{aligned}$$

Using the definition of the Shannon entropy $\mathcal{H} = -\mathbb{E}(\log_2 \mathcal{L})$ and applying Lemma 2 with function $f(x) = \frac{x^{\frac{1}{b-1}} \ln(x)(1-xb)}{b-1} + x^{\frac{b-d}{b-1}} (x \ln(x) + (1-x) \ln(1-x))$ finally gives

$$\begin{aligned} \mathcal{H} &= -\mathbb{E}(\log_2 \mathcal{L}) = -\frac{1}{\ln 2} \mathbb{E}(\ln \mathcal{L}) \\ &\approx \frac{m}{(\ln b)(\ln 2)} \int_0^1 z^{\frac{1}{b-1}-1} \frac{(1-zb)}{b-1} + z^{\frac{b-d}{b-1}} \left(1 + \frac{(1-z) \ln(1-z)}{z \ln z} \right) dz \\ &= \frac{m}{(\ln b)(\ln b)} \left(\left(1 + \frac{b-d}{b-1} \right)^{-1} + \int_0^1 z^{\frac{b-d}{b-1}} \frac{(1-z) \ln(1-z)}{z \ln z} dz \right). \end{aligned} \quad \square$$

LEMMA 6. The first-order bias of the ML estimate \hat{n}_{ML} for the distinct count n under the assumption of the simplified PMF (4) is roughly given by

$$\text{Bias}(\hat{n}_{\text{ML}}) \approx \frac{n}{m} \left(\frac{2b-d}{b-1} \right) \frac{\zeta \left(3, 1 + \frac{b-d}{b-1} \right)}{\left(\zeta \left(2, 1 + \frac{b-d}{b-1} \right) \right)^2}$$

where ζ denotes the Hurwitz zeta function as introduced in Lemma 4. The bias-corrected ML estimator is therefore given by

$$\hat{n}_{\text{ML}} \left(1 + \frac{1}{m} (\ln b) \left(1 + \frac{2b-d}{b-1} \right) \frac{\zeta \left(3, 1 + \frac{b-d}{b-1} \right)}{\left(\zeta \left(2, 1 + \frac{b-d}{b-1} \right) \right)^2} \right)^{-1}.$$

PROOF. The first-order bias of the ML estimator is given by [16]

$$\text{Bias}(\hat{n}_{\text{ML}}) \approx \frac{1}{I^2} \mathbb{E} \left(\frac{1}{2} \frac{\partial^3 \ln \mathcal{L}}{\partial n^3} + \frac{\partial^2 \ln \mathcal{L}}{\partial n^2} \frac{\partial \ln \mathcal{L}}{\partial n} \right).$$

We have

$$\begin{aligned} \mathbb{E}\left(\frac{\partial^3 \ln \mathcal{L}}{\partial n^3}\right) &= m \sum_{r=-\infty}^{\infty} \tilde{\rho}_{\text{reg}}(r|n) \frac{\partial^3 \ln \tilde{\rho}_{\text{reg}}(r|n)}{\partial n^3} \\ &= -\frac{m}{n^3} \sum_{u=-\infty}^{\infty} \sum_{l_1, \dots, l_d \in \{0,1\}} \tilde{\rho}_{\text{reg}}(u 2^d + \langle l_1 \dots l_d \rangle_2 | n) \cdot \\ &\quad \cdot \left(\frac{z_u(1+z_u) \ln^3 z_u}{(1-z_u)^3} + \sum_{j=1}^d l_j \frac{z_{u-j}(1+z_{u-j}) \ln^3 z_{u-j}}{(1-z_{u-j})^3} \right). \end{aligned}$$

Here we used (4) and Lemma 1 for the third-order derivatives. Using Lemma 3 leads to

$$\begin{aligned} \mathbb{E}\left(\frac{\partial^3 \ln \mathcal{L}}{\partial n^3}\right) &= -\frac{m}{n^3} \sum_{u=-\infty}^{\infty} z_u^{\frac{1}{b-1}} (1-z_u) \cdot \\ &\quad \cdot \left(\frac{z_u(1+z_u) \ln^3 z_u}{(1-z_u)^3} + \sum_{j=1}^d \frac{z_{u-j}(1+z_{u-j}) \ln^3 z_{u-j}}{(1-z_{u-j})^2} \right) \\ &= -\frac{m}{n^3} \sum_{u=-\infty}^{\infty} \left(\frac{z_u^{\frac{b}{b-1}} (1+z_u) \ln^3 z_u}{(1-z_u)^2} + \sum_{j=1}^d (z_{u+j}^{\frac{1}{b-1}} - z_{u+j-1}^{\frac{1}{b-1}}) \frac{z_u(1+z_u) \ln^3 z_u}{(1-z_u)^2} \right) \\ &= -\frac{m}{n^3} \sum_{u=-\infty}^{\infty} \left(z_u^{\frac{b}{b-1}} + (z_{u+d}^{\frac{1}{b-1}} - z_u^{\frac{1}{b-1}}) z_u \right) \frac{(1+z_u) \ln^3 z_u}{(1-z_u)^2} \\ &= -\frac{m}{n^3} \sum_{u=-\infty}^{\infty} \frac{z_u^{1+\frac{b-d}{b-1}} (1+z_u) \ln^3 z_u}{(1-z_u)^2}. \end{aligned}$$

Furthermore, we have

$$\begin{aligned} \mathbb{E}\left(\frac{\partial \ln \mathcal{L}}{\partial n} \frac{\partial^2 \ln \mathcal{L}}{\partial n^2}\right) &= m \sum_{r=-\infty}^{\infty} \tilde{\rho}_{\text{reg}}(r|n) \frac{\partial \ln \tilde{\rho}_{\text{reg}}(r|n)}{\partial n} \frac{\partial^2 \ln \tilde{\rho}_{\text{reg}}(r|n)}{\partial n^2} \\ &= -\frac{m}{n^3} \sum_{u=-\infty}^{\infty} \sum_{l_1, \dots, l_d \in \{0,1\}} \tilde{\rho}_{\text{reg}}(u 2^d + \langle l_1 \dots l_d \rangle_2 | n) \cdot \\ &\quad \cdot \left(\frac{\ln z_u}{b-1} - \frac{z_u \ln z_u}{1-z_u} + \sum_{j=1}^d (1-l_j) \ln z_{u-j} - l_j \frac{z_{u-j} \ln z_{u-j}}{1-z_{u-j}} \right) \\ &\quad \cdot \left(\frac{z_u \ln^2 z_u}{(1-z_u)^2} + \sum_{j=1}^d l_j \frac{z_{u-j} \ln^2 z_{u-j}}{(1-z_{u-j})^2} \right). \end{aligned}$$

Here we used (4) and Lemma 1 for the derivatives. Using again Lemma 3 together with $l_j(1-l_j) = 0$ and $l_j^2 = l_j$ gives

$$\begin{aligned} \mathbb{E}\left(\frac{\partial \ln \mathcal{L}}{\partial n} \frac{\partial^2 \ln \mathcal{L}}{\partial n^2}\right) &= -\frac{m}{n^3} \sum_{u=-\infty}^{\infty} z_u^{\frac{1}{b-1}} (1-z_u) \left(\frac{\ln z_u}{b-1} - \frac{z_u \ln z_u}{1-z_u} \right) \cdot \\ &\quad \cdot \left(\frac{z_u \ln^2 z_u}{(1-z_u)^2} + \sum_{j=1}^d \frac{z_{u-j} \ln^2 z_{u-j}}{1-z_{u-j}} \right) \\ &+ \frac{m}{n^3} \sum_{u=-\infty}^{\infty} z_u^{\frac{1}{b-1}} (1-z_u) \sum_{j=1}^d \frac{z_{u-j}^2 \ln^3 z_{u-j}}{(1-z_{u-j})^2} \end{aligned}$$

$$\begin{aligned} &= \frac{m}{n^3} \sum_{u=-\infty}^{\infty} z_u^{\frac{1}{b-1}} (1-z_u) \left(-\frac{\ln z_u}{b-1} + \frac{z_u \ln z_u}{1-z_u} \right) \cdot \\ &\quad \cdot \left(\frac{z_u \ln^2 z_u}{(1-z_u)^2} + \sum_{j=1}^d \frac{z_{u-j} \ln^2 z_{u-j}}{1-z_{u-j}} \right) \\ &+ \frac{m}{n^3} \sum_{u=-\infty}^{\infty} \sum_{j=1}^d (z_{u+j}^{\frac{1}{b-1}} - z_{u+j-1}^{\frac{1}{b-1}}) \frac{z_u^2 \ln^3 z_u}{(1-z_u)^2} \\ &\quad \left(z_u^{\frac{1}{b-1}} \frac{z_u^2 \ln^3 z_u}{(1-z_u)^2} + z_u^{\frac{1}{b-1}} z_u (\ln z_u) \left(\sum_{j=1}^d \frac{z_{u-j} \ln^2 z_{u-j}}{1-z_{u-j}} \right) \right) \\ &= \frac{m}{n^3} \sum_{u=-\infty}^{\infty} \left(\begin{array}{l} -\frac{z_u^{\frac{1}{b-1}}}{b-1} \frac{z_u \ln^3 z_u}{1-z_u} \\ -z_u^{\frac{1}{b-1}} (1-z_u) \frac{\ln z_u}{b-1} \left(\sum_{j=1}^d \frac{z_{u-j} \ln^2 z_{u-j}}{1-z_{u-j}} \right) \\ + z_u^{\frac{1}{b-1}} \frac{z_u^2 \ln^3 z_u}{(1-z_u)^2} - z_u^{\frac{1}{b-1}} \frac{z_u^2 \ln^3 z_u}{(1-z_u)^2} \end{array} \right) \\ &= \frac{m}{n^3} \sum_{u=-\infty}^{\infty} \left(\begin{array}{l} \frac{z_u \ln^3 z_u}{1-z_u} \left(\frac{z_{u+d}^{\frac{1}{b-1}} z_u}{1-z_u} - \frac{z_u^{\frac{1}{b-1}}}{b-1} \right) \\ + z_u^{\frac{1}{b-1}} \ln z_u \left(z_u - \frac{1-z_u}{b-1} \right) \left(\sum_{j=1}^d \frac{z_{u-j} \ln^2 z_{u-j}}{1-z_{u-j}} \right) \end{array} \right) \\ &= \frac{m}{n^3} \sum_{u=-\infty}^{\infty} \left(\begin{array}{l} \frac{z_u \ln^3 z_u}{1-z_u} \left(\frac{z_u^{\frac{b-d}{b-1}} z_u}{1-z_u} - \frac{z_u^{\frac{1}{b-1}}}{b-1} \right) \\ + \sum_{j=1}^d z_{u+j}^{\frac{1}{b-1}} \ln z_{u+j} \left(z_{u+j} - \frac{1-z_{u+j}}{b-1} \right) \frac{z_u \ln^2 z_u}{1-z_u} \end{array} \right) \\ &= \frac{m}{n^3} \sum_{u=-\infty}^{\infty} \left(\begin{array}{l} \frac{z_u \ln^3 z_u}{1-z_u} \left(\frac{z_u^{\frac{b-d}{b-1}} z_u}{1-z_u} - \frac{z_u^{\frac{1}{b-1}}}{b-1} \right) \\ + \sum_{j=1}^d z_u^{\frac{b-j}{b-1}} \ln(z_u^{b-j}) \left(z_u^{b-j} - \frac{1-z_u^{b-j}}{b-1} \right) \frac{z_u \ln^2 z_u}{1-z_u} \end{array} \right) \\ &= \frac{m}{n^3} \sum_{u=-\infty}^{\infty} \frac{z_u \ln^3 z_u}{1-z_u} \cdot \\ &\quad \cdot \left(\frac{z_u^{\frac{b-d}{b-1}} z_u}{1-z_u} - \frac{z_u^{\frac{1}{b-1}}}{b-1} + \sum_{j=1}^d z_u^{\frac{b-j}{b-1}} b^{-j} \left(z_u^{b-j} - \frac{1-z_u^{b-j}}{b-1} \right) \right) \\ &= \frac{m}{n^3} \sum_{u=-\infty}^{\infty} \frac{z_u \ln^3 z_u}{1-z_u} \cdot \\ &\quad \cdot \left(\frac{z_u^{\frac{b-d}{b-1}} z_u}{1-z_u} - \frac{z_u^{\frac{1}{b-1}}}{b-1} + \sum_{j=1}^d \frac{z_u^{\frac{b-j+1}{b-1}} b^{-j+1}}{b-1} - \frac{z_u^{\frac{b-j}{b-1}} b^{-j}}{b-1} \right) \\ &= \frac{m}{n^3} \sum_{u=-\infty}^{\infty} \frac{z_u \ln^3 z_u}{1-z_u} \left(\frac{z_u^{\frac{b-d}{b-1}} z_u}{1-z_u} - \frac{z_u^{\frac{b-d}{b-1}} b^{-d}}{b-1} \right) \\ &= \frac{m}{n^3} \sum_{u=-\infty}^{\infty} \frac{z_u^{\frac{b-d}{b-1}} z_u \ln^3 z_u}{1-z_u} \left(\frac{z_u}{1-z_u} - \frac{b^{-d}}{b-1} \right) \\ &= \frac{m}{n^3} \sum_{u=-\infty}^{\infty} \frac{z_u^{1+\frac{b-d}{b-1}} \ln^3 z_u}{(1-z_u)^2} \left(z_u \left(1 + \frac{b^{-d}}{b-1} \right) - \frac{b^{-d}}{b-1} \right). \end{aligned}$$

Therefore, we get

$$\begin{aligned}
\text{Bias}(\hat{n}_{\text{ML}}) &\approx \frac{1}{I^2} \mathbb{E} \left(\frac{1}{2} \frac{\partial^3 \ln \mathcal{L}}{\partial n^3} + \frac{\partial^2 \ln \mathcal{L}}{\partial n^2} \frac{\partial \ln \mathcal{L}}{\partial n} \right) \\
&= \frac{1}{I^2} \frac{m}{n^3} \left(\sum_{u=-\infty}^{\infty} -\frac{1}{2} \frac{z_u^{1+\frac{b-d}{b-1}} (1+z_u) \ln^3 z_u}{(1-z_u)^2} \right. \\
&\quad \left. + \sum_{u=-\infty}^{\infty} \frac{z_u^{1+\frac{b-d}{b-1}} \ln^3 z_u}{(1-z_u)^2} \left(z_u \left(1 + \frac{b-d}{b-1} \right) - \frac{b-d}{b-1} \right) \right) \\
&= -\frac{1}{I^2} \frac{m}{n^3} \sum_{u=-\infty}^{\infty} \frac{z_u^{1+\frac{b-d}{b-1}} \ln^3 z_u}{(1-z_u)^2} \left(\frac{1+z_u}{2} - z_u \left(1 + \frac{b-d}{b-1} \right) + \frac{b-d}{b-1} \right) \\
&= -\frac{1}{I^2} \frac{m}{n^3} \left(\frac{1}{2} + \frac{b-d}{b-1} \right) \sum_{u=-\infty}^{\infty} \frac{z_u^{1+\frac{b-d}{b-1}} \ln^3 z_u}{1-z_u}.
\end{aligned}$$

Lemma 2 with $f(x) = \frac{x^{1+\frac{b-d}{b-1}} \ln^3 x}{1-x}$ yields

$$\begin{aligned}
\text{Bias}(\hat{n}_{\text{ML}}) &\approx \frac{1}{I^2} \frac{m}{n^3} \left(\frac{1}{2} + \frac{b-d}{b-1} \right) \frac{1}{\ln b} \int_0^{\infty} \frac{e^{-y(1+\frac{b-d}{b-1})} y^2}{1-e^{-y}} dy \\
&= \frac{1}{I^2} \frac{m}{n^3} \left(1 + \frac{2b-d}{b-1} \right) \frac{1}{\ln b} \zeta \left(3, 1 + \frac{b-d}{b-1} \right).
\end{aligned}$$

Replacing I by using Lemma 4 finally gives

$$\text{Bias}(\hat{n}_{\text{ML}}) \approx \frac{n}{m} (\ln b) \left(1 + \frac{2b-d}{b-1} \right) \frac{\zeta(3, 1 + \frac{b-d}{b-1})}{\left(\zeta(2, 1 + \frac{b-d}{b-1}) \right)^2}.$$

□

LEMMA 7. For a random variable r distributed according to (4), the expectation of

$$g(r) = \kappa b^{-\tau u} \left(\frac{1}{b^\tau - 1} + \sum_{s=1}^d (1-l_s) b^{s\tau} \right)$$

with $r = u2^d + \langle l_1 \dots l_d \rangle_2$ and $\kappa = \frac{(b-1+b-d)^\tau \ln b}{\Gamma(\tau)}$ can be approximated using Lemma 2 by

$$\mathbb{E}(g(r)) \approx \frac{m^\tau}{n^\tau}.$$

PROOF. Using (4) the expectation can be expressed as

$$\begin{aligned}
\mathbb{E}(g(r)) &= \sum_{r=-\infty}^{\infty} \tilde{\rho}_{\text{reg}}(r|n) g(r) \\
&= \sum_{u=-\infty}^{\infty} \kappa b^{-\tau u} \sum_{l_1, \dots, l_d \in \{0,1\}} \tilde{\rho}_{\text{reg}}(u2^d + \langle l_1 \dots l_d \rangle_2 | n) \\
&\quad \cdot \left(\frac{1}{b^\tau - 1} + \sum_{s=1}^d (1-l_s) b^{s\tau} \right).
\end{aligned}$$

With the help of Lemma 3 we get

$$\begin{aligned}
\mathbb{E}(g(r)) &= \sum_{u=-\infty}^{\infty} \kappa b^{-\tau u} z_u^{\frac{1}{b-1}} (1-z_u) \left(\frac{1}{b^\tau - 1} + \sum_{s=1}^d z_{u-s} b^{s\tau} \right)
\end{aligned}$$

$$\begin{aligned}
&= \kappa \sum_{u=-\infty}^{\infty} \frac{b^{-\tau u} z_u^{\frac{1}{b-1}} (1-z_u)}{b^\tau - 1} + \sum_{s=1}^d \left(z_{u-s}^{1+\frac{b-s}{b-1}} - z_{u-s}^{1+\frac{b^{1-s}}{b-1}} \right) b^{\tau(s-u)} \\
&= \kappa \sum_{u=-\infty}^{\infty} \frac{b^{-\tau u} z_u^{\frac{1}{b-1}} (1-z_u)}{b^\tau - 1} + \sum_{s=1}^d \left(z_u^{1+\frac{b-s}{b-1}} - z_u^{1+\frac{b^{1-s}}{b-1}} \right) b^{-\tau u} \\
&= \kappa \sum_{u=-\infty}^{\infty} b^{-\tau u} \left(\frac{z_u^{\frac{1}{b-1}} (1-z_u)}{b^\tau - 1} + z_u^{1+\frac{b-d}{b-1}} - z_u^{1+\frac{1}{b-1}} \right) \\
&= \frac{\kappa m^\tau}{n^\tau (b-1)^\tau} \sum_{u=-\infty}^{\infty} (-\ln z_u)^\tau \left(\frac{z_u^{\frac{1}{b-1}} (1-z_u)}{b^\tau - 1} + z_u^{1+\frac{b-d}{b-1}} - z_u^{1+\frac{1}{b-1}} \right) \\
&= \frac{\kappa m^\tau}{n^\tau (b-1)^\tau} \left(\sum_{u=-\infty}^{\infty} (-\ln z_u)^\tau z_u^{1+\frac{b-d}{b-1}} \right) \\
&\quad + \frac{\kappa m^\tau}{n^\tau (b-1)^\tau} \left(\sum_{u=-\infty}^{\infty} \frac{(-\ln z_u)^\tau z_u^{\frac{1}{b-1}}}{b^\tau - 1} - \frac{(-\ln z_u)^\tau z_u^{\frac{1}{b-1}}}{b^\tau - 1} \right) \\
&= \frac{\kappa m^\tau}{n^\tau (b-1)^\tau} \left(\sum_{u=-\infty}^{\infty} (-\ln z_u)^\tau z_u^{1+\frac{b-d}{b-1}} \right) \\
&\quad + \frac{\kappa m^\tau}{n^\tau (b-1)^\tau} \left(\sum_{u=-\infty}^{\infty} \frac{(-\ln z_u)^\tau z_u^{\frac{1}{b-1}}}{b^\tau - 1} - \frac{(-\ln z_{u-1})^\tau z_{u-1}^{\frac{1}{b-1}}}{b^\tau - 1} \right) \\
&= \frac{\kappa m^\tau}{n^\tau (b-1)^\tau} \sum_{u=-\infty}^{\infty} (-\ln z_u)^\tau z_u^{1+\frac{b-d}{b-1}}.
\end{aligned}$$

The approximation given in Lemma 2 and the identity $\int_0^{\infty} y^{\tau-1} e^{-yx} dy = \frac{\Gamma(\tau)}{x^\tau}$ finally leads to

$$\begin{aligned}
\mathbb{E}(g(r)) &\approx \frac{\kappa m^\tau}{n^\tau (b-1)^\tau \ln b} \int_0^{\infty} y^{\tau-1} e^{-y(1+\frac{b-d}{b-1})} dy \\
&= \frac{\kappa m^\tau \Gamma(\tau)}{n^\tau (b-1+b-d)^\tau \ln b} = \frac{m^\tau}{n^\tau}.
\end{aligned}$$

□

LEMMA 8. For a random variable r distributed according to (4), the expectation of $(g(r))^2$ with $g(r)$ as defined in Lemma 7 can be approximated using Lemma 2 by

$$\mathbb{E}((g(r))^2)$$

$$\approx \frac{m^{2\tau} \Gamma(2\tau) \ln b}{n^{2\tau} (\Gamma(\tau))^2} \left(1 + \frac{2b^{-\tau d}}{b^\tau - 1} + \sum_{s=1}^d \frac{2b^{-\tau s}}{\left(1 + \frac{(b-1)^{b-s}}{b-1+b-d} \right)^{2\tau}} \right).$$

PROOF. Since $l_s \in \{0, 1\}$, we have $(1-l_s) = (1-l_s)^2$ and we can write

$$\begin{aligned}
(g(r))^2 &= \kappa^2 b^{-2\tau u} \left(\frac{1}{b^\tau - 1} + \sum_{s=1}^d (1-l_s) b^{s\tau} \right)^2 \\
&= \kappa^2 b^{-2\tau u} \left(\frac{1}{(b^\tau - 1)^2} + \sum_{s=1}^d (1-l_s) \left(\frac{2b^{s\tau}}{b^\tau - 1} + b^{2s\tau} \right) \right. \\
&\quad \left. + 2 \sum_{s=1}^{d-1} (1-l_s) \sum_{s'=1}^{d-s} b^{\tau(2s+s')} (1-l_{s+s'}) \right).
\end{aligned}$$

Using (4) the expectation can be expressed as

$$\mathbb{E}((g(r))^2) = \sum_{r=-\infty}^{\infty} \tilde{\rho}_{\text{reg}}(r|n) (g(r))^2$$

$$\begin{aligned}
&= \sum_{u=-\infty}^{\infty} \sum_{l_1, \dots, l_d \in \{0,1\}} \kappa^2 b^{-2\tau u} \tilde{\rho}_{\text{reg}}(u2^d + \langle l_1 \dots l_d \rangle_2 | n) \cdot \\
&\quad \cdot \begin{pmatrix} \frac{1}{(b^{\tau}-1)^2} + \sum_{s=1}^d (1-l_s) \left(\frac{2b^{\tau s}}{b^{\tau}-1} + b^{2\tau s} \right) \\ + 2 \sum_{s=1}^{d-1} (1-l_s) \sum_{s'=1}^{d-s} b^{\tau(2s+s')} (1-l_{s+s'}) \end{pmatrix}.
\end{aligned}$$

Lemma 3 allows to write that as

$$\begin{aligned}
\mathbb{E}((g(r))^2) &= \sum_{u=-\infty}^{\infty} \kappa^2 b^{-2\tau u} z_u^{\frac{1}{b-1}} (1-z_u) \cdot \\
&\quad \cdot \begin{pmatrix} \frac{1}{(b^{\tau}-1)^2} + \sum_{s=1}^d z_{u-s} \left(\frac{2b^{\tau s}}{b^{\tau}-1} + b^{2\tau s} \right) \\ + 2 \sum_{s=1}^{d-1} z_{u-s} \sum_{s'=1}^{d-s} b^{\tau(2s+s')} z_{u-s-s'} \end{pmatrix} \\
&= \sum_{u=-\infty}^{\infty} \kappa^2 b^{-2\tau u} (z_u^{\frac{1}{b-1}} - z_{u-1}^{\frac{1}{b-1}}) \cdot \\
&\quad \cdot \begin{pmatrix} \frac{1}{(b^{\tau}-1)^2} + \sum_{s=1}^d z_{u-s} \left(\frac{2b^{\tau s}}{b^{\tau}-1} + b^{2\tau s} \right) \\ + 2 \sum_{s=1}^{d-1} \sum_{s'=1}^{d-s} b^{\tau(2s+s')} z_{u-s} z_{u-s-s'} \end{pmatrix} \\
&= \sum_{u=-\infty}^{\infty} \kappa^2 b^{-2\tau u} z_u^{\frac{1}{b-1}} \cdot \\
&\quad \cdot \begin{pmatrix} \frac{1-b^{-2\tau}}{(b^{\tau}-1)^2} + \sum_{s=1}^d (z_{u-s} - z_{u+1-s} b^{-2\tau}) \left(\frac{2b^{\tau s}}{b^{\tau}-1} + b^{2\tau s} \right) \\ + 2 \sum_{s=1}^{d-1} \sum_{s'=1}^{d-s} \begin{pmatrix} b^{\tau(2s+s')} z_{u-s} z_{u-s-s'} \\ - b^{\tau(2s+s'-2)} z_{u+1-s} z_{u+1-s-s'} \end{pmatrix} \end{pmatrix} \\
&= \sum_{u=-\infty}^{\infty} \kappa^2 b^{-2\tau u} z_u^{\frac{1}{b-1}} \cdot \\
&\quad \cdot \begin{pmatrix} b^{-2\tau} \frac{b^{\tau}+1}{b^{\tau}-1} + \sum_{s=1}^d (z_{u-s} - z_{u+1-s} b^{-2\tau}) \frac{2b^{\tau s}}{b^{\tau}-1} \\ + \sum_{s=1}^d (z_{u-s} b^{2\tau s} - z_{u-(s-1)} b^{2\tau(s-1)}) \\ + 2 \sum_{s=1}^{d-1} \sum_{s'=1}^{d-s} \begin{pmatrix} b^{\tau(2s+s')} z_{u-s} z_{u-s-s'} \\ - b^{\tau(2(s-1)+s')} z_{u-(s-1)} z_{u-(s-1)-s'} \end{pmatrix} \end{pmatrix} \\
&= \sum_{u=-\infty}^{\infty} \kappa^2 b^{-2\tau u} z_u^{\frac{1}{b-1}} \cdot \\
&\quad \cdot \begin{pmatrix} b^{-2\tau} \frac{b^{\tau}+1}{b^{\tau}-1} \\ + \sum_{s=1}^d (z_{u-s} - z_{u+1-s} b^{-2\tau}) \frac{2b^{\tau s}}{b^{\tau}-1} \\ + z_{u-d} b^{2\tau d} - z_u \\ + 2 \sum_{s'=1}^{d-1} \begin{pmatrix} b^{\tau(2d-s')} z_{u-d+s'} z_{u-d} \\ - b^{\tau s'} z_u z_{u-s'} \end{pmatrix} \end{pmatrix} \\
&= \sum_{u=-\infty}^{\infty} \kappa^2 b^{-2\tau u} \left(z_u^{\frac{1}{b-1}} b^{-2\tau} \frac{b^{\tau}+1}{b^{\tau}-1} + z_u^{\frac{1}{b-1}} z_{u-d} b^{2\tau d} - z_u^{\frac{1}{b-1}} z_u \right. \\
&\quad \left. + z_u^{\frac{1}{b-1}} \sum_{s=1}^d (z_{u-s} - z_{u+1-s} b^{-2\tau}) \frac{2b^{\tau s}}{b^{\tau}-1} \right. \\
&\quad \left. + 2 z_u^{\frac{1}{b-1}} \sum_{s=1}^d \begin{pmatrix} b^{\tau(2d-s)} z_{u-d+s} z_{u-d} \\ - b^{\tau s} z_u z_{u-s} \end{pmatrix} \right) \\
&= \sum_{u=-\infty}^{\infty} \kappa^2 b^{-2\tau u} \cdot \\
&\quad \cdot \begin{pmatrix} z_u^{\frac{b}{b-1}} \frac{b^{\tau}+1}{b^{\tau}-1} + z_u^{1+\frac{b-d}{b-1}} - z_u^{\frac{b}{b-1}} \\ + 2 \sum_{s=1}^d \begin{pmatrix} z_u^{\frac{1}{b-1}} z_{u-s} - z_u^{\frac{1}{b-1}} z_{u+1-s} b^{-2\tau} \frac{b^{\tau s}}{b^{\tau}-1} \\ + 2 \sum_{s=1}^d \begin{pmatrix} z_u^{\frac{1}{b-1}} b^{\tau s} z_{u-s} - z_u^{\frac{1}{b-1}} b^{\tau(s+1)} z_{u-s} \end{pmatrix} \end{pmatrix} \\
&+ 2 \sum_{s=1}^d z_{u+d}^{\frac{1}{b-1}} b^{-\tau s} z_{u+s} z_u \end{pmatrix} \\
&= \sum_{u=-\infty}^{\infty} \kappa^2 b^{-2\tau u} \cdot \\
&\quad \cdot \begin{pmatrix} z_u^{\frac{b}{b-1}} \frac{b^{\tau}+1}{b^{\tau}-1} + z_u^{1+\frac{b-d}{b-1}} \\ + \frac{2}{b^{\tau}-1} \sum_{s=1}^d \begin{pmatrix} z_u^{\frac{1}{b-1}} z_{u-s} b^{\tau s} - z_u^{\frac{1}{b-1}} b^{\tau(s-1)} z_{u-(s-1)} \end{pmatrix} \\
+ 2 \sum_{s=1}^d z_{u+d}^{\frac{1}{b-1}} b^{-\tau s} z_{u+s} z_u \end{pmatrix} \\
&= \sum_{u=-\infty}^{\infty} \kappa^2 b^{-2\tau u} \left(z_u^{\frac{b}{b-1}} \frac{b^{\tau}+1}{b^{\tau}-1} + z_u^{1+\frac{b-d}{b-1}} \right. \\
&\quad \left. + 2 \sum_{s=1}^d z_{u+d}^{\frac{1}{b-1}} b^{-\tau s} z_{u+s} z_u \right) \\
&= \sum_{u=-\infty}^{\infty} \kappa^2 b^{-2\tau u} \left(1 + \frac{2b^{-\tau d}}{b^{\tau}-1} \right) \sum_{u=-\infty}^{\infty} z_u^{1+\frac{b-d}{b-1}} b^{-2\tau u} \\
&\quad + 2\kappa^2 \sum_{s=1}^d b^{-\tau s} \sum_{u=-\infty}^{\infty} z_u^{1+\frac{b-d}{b-1}+b^{-s}} b^{-2\tau u} \\
&= \frac{m^{2\tau} \kappa^2 \left(1 + \frac{2b^{-\tau d}}{b^{\tau}-1} \right)}{n^{2\tau} (b-1)^{2\tau}} \sum_{u=-\infty}^{\infty} z_u^{1+\frac{b-d}{b-1}} (-\ln z_u)^{2\tau} \\
&\quad + \frac{2m^{2\tau} \kappa^2}{n^{2\tau} (b-1)^{2\tau}} \sum_{s=1}^d b^{-\tau s} \sum_{u=-\infty}^{\infty} z_u^{1+\frac{b-d}{b-1}+b^{-s}} (-\ln z_u)^{2\tau}.
\end{aligned}$$

$$\begin{aligned}
&\left. \begin{pmatrix} z_u^{\frac{b}{b-1}} \frac{2}{b^{\tau}-1} + z_u^{1+\frac{b-d}{b-1}} \\ + 2 \sum_{s=1}^d \begin{pmatrix} z_u^{\frac{1}{b-1}} z_{u-s} - z_u^{\frac{1}{b-1}} z_{u+1-s} b^{-2\tau} \frac{b^{\tau s}}{b^{\tau}-1} \\ + z_u^{\frac{1}{b-1}} b^{\tau s} z_{u-s} - z_u^{\frac{1}{b-1}} b^{\tau(s+1)} z_{u-s} \end{pmatrix} \end{pmatrix} \right) \\
&= \sum_{u=-\infty}^{\infty} \kappa^2 b^{-2\tau u} \cdot \\
&\quad \cdot \begin{pmatrix} z_u^{\frac{b}{b-1}} \frac{2}{b^{\tau}-1} + z_u^{1+\frac{b-d}{b-1}} \\ + \frac{2}{b^{\tau}-1} \sum_{s=1}^d \begin{pmatrix} z_u^{\frac{1}{b-1}} z_{u-s} b^{\tau s} - z_u^{\frac{1}{b-1}} z_{u+1-s} b^{\tau(s-2)} \\ + z_u^{\frac{1}{b-1}} b^{\tau s} z_{u-s} - z_u^{\frac{1}{b-1}} b^{\tau(s+1)} z_{u-s} \end{pmatrix} \\
+ 2 \sum_{s=1}^d z_{u+d}^{\frac{1}{b-1}} b^{-\tau s} z_{u+s} z_u \end{pmatrix} \\
&= \sum_{u=-\infty}^{\infty} \kappa^2 b^{-2\tau u} \cdot \\
&\quad \cdot \begin{pmatrix} z_u^{\frac{b}{b-1}} \frac{2}{b^{\tau}-1} + z_u^{1+\frac{b-d}{b-1}} \\ + \frac{2}{b^{\tau}-1} \sum_{s=1}^d \begin{pmatrix} z_u^{\frac{1}{b-1}} z_{u-s} b^{\tau s} - z_u^{\frac{1}{b-1}} z_{u-s} b^{\tau s} \\ + z_u^{\frac{1}{b-1}} b^{\tau s} z_{u-s} - z_u^{\frac{1}{b-1}} b^{\tau(s+1)} z_{u-s} \end{pmatrix} \\
+ 2 \sum_{s=1}^d z_{u+d}^{\frac{1}{b-1}} b^{-\tau s} z_{u+s} z_u \end{pmatrix} \\
&= \sum_{u=-\infty}^{\infty} \kappa^2 b^{-2\tau u} \cdot \\
&\quad \cdot \begin{pmatrix} z_u^{\frac{b}{b-1}} \frac{2}{b^{\tau}-1} + z_u^{1+\frac{b-d}{b-1}} \\ + \frac{2}{b^{\tau}-1} \sum_{s=1}^d \begin{pmatrix} z_u^{\frac{1}{b-1}} z_{u-d} b^{\tau d} - z_u^{\frac{1}{b-1}} z_u \\ + z_u^{\frac{1}{b-1}} z_{u-d} b^{-\tau s} z_{u+s} z_u \end{pmatrix} \\
+ 2 \sum_{s=1}^d z_{u+d}^{\frac{1}{b-1}} b^{-\tau s} z_{u+s} z_u \end{pmatrix} \\
&= \sum_{u=-\infty}^{\infty} \kappa^2 b^{-2\tau u} \left(z_u^{1+\frac{b-d}{b-1}} + \frac{2}{b^{\tau}-1} z_{u+d}^{\frac{1}{b-1}} z_u b^{-\tau d} \right) \\
&= \kappa^2 \left(1 + \frac{2b^{-\tau d}}{b^{\tau}-1} \right) \sum_{u=-\infty}^{\infty} z_u^{1+\frac{b-d}{b-1}} b^{-2\tau u} \\
&\quad + 2\kappa^2 \sum_{s=1}^d b^{-\tau s} \sum_{u=-\infty}^{\infty} z_u^{1+\frac{b-d}{b-1}+b^{-s}} b^{-2\tau u} \\
&= \frac{m^{2\tau} \kappa^2 \left(1 + \frac{2b^{-\tau d}}{b^{\tau}-1} \right)}{n^{2\tau} (b-1)^{2\tau}} \sum_{u=-\infty}^{\infty} z_u^{1+\frac{b-d}{b-1}} (-\ln z_u)^{2\tau} \\
&\quad + \frac{2m^{2\tau} \kappa^2}{n^{2\tau} (b-1)^{2\tau}} \sum_{s=1}^d b^{-\tau s} \sum_{u=-\infty}^{\infty} z_u^{1+\frac{b-d}{b-1}+b^{-s}} (-\ln z_u)^{2\tau}.
\end{aligned}$$

The approximation given in Lemma 2 and the identity $\int_0^\infty e^{-xy} y^{2\tau-1} dy = \frac{\Gamma(2\tau)}{x^{2\tau}}$ finally leads to

$$\begin{aligned} \mathbb{E}((g(r))^2) &\approx \frac{m^{2\tau} \kappa^2 \left(1 + \frac{2b^{-\tau d}}{b^{\tau-1}}\right)}{n^{2\tau} (b-1)^{2\tau} \ln b} \int_0^\infty e^{-y(1+\frac{b^{-d}}{b-1})} y^{2\tau-1} dy \\ &+ \frac{2m^{2\tau} \kappa^2}{n^{2\tau} (b-1)^{2\tau} \ln b} \sum_{s=1}^d b^{-\tau s} \int_0^\infty e^{-y(1+\frac{b^{-d}}{b-1}+b^{-s})} y^{2\tau-1} dy \\ &= \frac{m^{2\tau} \kappa^2 \Gamma(2\tau)}{n^{2\tau} (b-1)^{2\tau} \ln b} \left(\frac{1 + \frac{2b^{-\tau d}}{b^{\tau-1}}}{(1 + \frac{b^{-d}}{b-1})^{2\tau}} + \sum_{s=1}^d \frac{2b^{-\tau s}}{(1 + \frac{b^{-d}}{b-1} + b^{-s})^{2\tau}} \right) \\ &= \frac{m^{2\tau} \Gamma(2\tau) \ln b}{n^{2\tau} (\Gamma(\tau))^2} \left(1 + \frac{2b^{-\tau d}}{b^{\tau-1}} + \sum_{s=1}^d \frac{2b^{-\tau s}}{\left(1 + \frac{(b-1)b^{-s}}{b-1+b^{-d}}\right)^{2\tau}} \right). \end{aligned}$$

□

LEMMA 9. For a random variable r that is distributed according to (4) with $d = 2$, the expectation of $g(r) = b^{-\tau \lfloor r/4 \rfloor} \eta_{r \bmod 4}$ with $\eta_0, \eta_1, \eta_2, \eta_3$ normalized by the condition

$$\eta_0 \omega_0(\tau) + \eta_1 \omega_1(\tau) + \eta_2 \omega_2(\tau) + \eta_3 \omega_3(\tau) = \frac{\ln b}{\Gamma(\tau)} \quad (26)$$

can be approximated with Lemma 2 by

$$\mathbb{E}(g(r)) \approx \frac{m^\tau}{n^\tau}.$$

$\omega_0(\tau), \omega_1(\tau), \omega_2(\tau)$, and $\omega_3(\tau)$ are positive functions for $b > 1, \tau > 0$ and defined by

$$\begin{aligned} \omega_0(\tau) &:= \frac{1}{(b^3-b+1)^\tau} - \frac{1}{b^{3\tau}}, \\ \omega_1(\tau) &:= \frac{1}{(b^2-b+1)^\tau} - \frac{1}{b^{2\tau}} - \frac{1}{(b^3-b+1)^\tau} + \frac{1}{b^{3\tau}}, \\ \omega_2(\tau) &:= \frac{1}{(b^3-b^2+1)^\tau} - \frac{1}{(b^3-b^2+b)^\tau} - \frac{1}{(b^3-b+1)^\tau} + \frac{1}{b^{3\tau}}, \\ \omega_3(\tau) &:= \frac{1}{(b^3-b+1)^\tau} - \frac{1}{(b^3-b^2+1)^\tau} + \frac{1}{(b^3-b^2+b)^\tau} - \frac{1}{b^{3\tau}} \\ &\quad - \frac{1}{(b^2-b+1)^\tau} + \frac{1}{b^{2\tau}} + 1 - \frac{1}{b^\tau}. \end{aligned}$$

PROOF. For $d = 2$ (4) can be written as

$$\tilde{\rho}_{\text{reg}}(r|n) = z_u^{\frac{1}{b-1}} (1 - z_u) z_{u-1}^{1-l_1} (1 - z_{u-1})^{l_1} z_{u-2}^{1-l_2} (1 - z_{u-2})^{l_2}$$

with $r = 4u + \langle l_1 l_2 \rangle_2$. The expectation of $g(r)$ is

$$\begin{aligned} \mathbb{E}(g(r)) &= \sum_{r=-\infty}^{\infty} \tilde{\rho}_{\text{reg}}(r|n) g(r) \\ &= \sum_{u=-\infty}^{\infty} \sum_{l_1=0}^1 \sum_{l_2=0}^1 \tilde{\rho}_{\text{reg}}(4u + \langle l_1 l_2 \rangle_2|n) g(4u + \langle l_1 l_2 \rangle_2) \\ &= \sum_{u=-\infty}^{\infty} z_u^{\frac{1}{b-1}} (1 - z_u) b^{-\tau u} \begin{pmatrix} z_{u-1} z_{u-2} \eta_0 + z_{u-1} (1 - z_{u-2}) \eta_1 \\ +(1 - z_{u-1}) z_{u-2} \eta_2 \\ +(1 - z_{u-1}) (1 - z_{u-2}) \eta_3 \end{pmatrix} \\ &= \frac{m^\tau}{n^\tau (b-1)^\tau} \sum_{u=-\infty}^{\infty} z_u^{\frac{1}{b-1}} (1 - z_u) (-\ln z_u)^\tau \\ &\quad \cdot \begin{pmatrix} z_u^{b(b+1)} \eta_0 + z_u^b (1 - z_u^{b^2}) \eta_1 \\ +(1 - z_u^b) z_u^{b^2} \eta_2 + (1 - z_u^b) (1 - z_u^{b^2}) \eta_3 \end{pmatrix} \end{aligned}$$

$$\begin{aligned} &= \frac{m^\tau}{n^\tau (b-1)^\tau} \sum_{u=-\infty}^{\infty} z_u^{\frac{1}{b-1}} (1 - z_u) (-\ln z_u)^\tau \\ &\quad \cdot \begin{pmatrix} z_u^{b(b+1)} (\eta_0 - \eta_1 - \eta_2 + \eta_3) + z_u^{b^2} (\eta_2 - \eta_3) + z_u^b (\eta_1 - \eta_3) + \eta_3 \end{pmatrix}. \end{aligned}$$

Lemma 2 with

$$f(x) = x^{\frac{1}{b-1}} (-\ln x)^\tau (1 - x) \begin{pmatrix} x^{b(b+1)} (\eta_0 - \eta_1 - \eta_2 + \eta_3) \\ + x^{b^2} (\eta_2 - \eta_3) + x^b (\eta_1 - \eta_3) + \eta_3 \end{pmatrix}$$

yields

$$\begin{aligned} \mathbb{E}(g(r)) &\approx \frac{m^\tau}{n^\tau (b-1)^\tau \ln b} \int_0^\infty e^{-y^{\frac{1}{b-1}}} (1 - e^{-y}) y^{\tau-1} \\ &\quad \cdot \begin{pmatrix} e^{-b(b+1)y} (\eta_0 - \eta_1 - \eta_2 + \eta_3) \\ + e^{-b^2 y} (\eta_2 - \eta_3) + e^{-b y} (\eta_1 - \eta_3) + \eta_3 \end{pmatrix} dy. \end{aligned}$$

Using $\int_0^\infty e^{-zy} (1 - e^{-y}) y^{\tau-1} dy = \frac{\Gamma(\tau)}{z^\tau} - \frac{\Gamma(\tau)}{(z+1)^\tau}$ gives

$$\begin{aligned} \mathbb{E}(g(r)) &\approx \frac{m^\tau \Gamma(\tau)}{n^\tau (b-1)^\tau \ln b} \cdot \begin{pmatrix} (\eta_0 - \eta_1 - \eta_2 + \eta_3) \cdot \\ \cdot \left(\left(\frac{1}{b-1} + b(b+1) \right)^{-\tau} - \left(\frac{b}{b-1} + b(b+1) \right)^{-\tau} \right) \\ + (\eta_2 - \eta_3) \left(\left(\frac{1}{b-1} + b^2 \right)^{-\tau} - \left(\frac{b}{b-1} + b^2 \right)^{-\tau} \right) \\ + (\eta_1 - \eta_3) \left(\left(\frac{1}{b-1} + b \right)^{-\tau} - \left(\frac{b}{b-1} + b \right)^{-\tau} \right) \\ + \eta_3 \left(\left(\frac{1}{b-1} \right)^{-\tau} - \left(\frac{b}{b-1} \right)^{-\tau} \right) \end{pmatrix} \\ &= \frac{m^\tau \Gamma(\tau)}{n^\tau \ln b} \begin{pmatrix} (\eta_0 - \eta_1 - \eta_2 + \eta_3) ((b^3 - b + 1)^{-\tau} - b^{-3\tau}) \\ + (\eta_2 - \eta_3) ((b^3 - b^2 + 1)^{-\tau} - (b^3 - b^2 + b)^{-\tau}) \\ + (\eta_1 - \eta_3) ((b^2 - b + 1)^{-\tau} - b^{-2\tau}) \\ + \eta_3 (1 - b^{-\tau}) \end{pmatrix} \\ &= \frac{m^\tau \Gamma(\tau)}{n^\tau \ln b} (\eta_0 \omega_0(\tau) + \eta_1 \omega_1(\tau) + \eta_2 \omega_2(\tau) + \eta_3 \omega_3(\tau)) = \frac{m^\tau}{n^\tau}. \end{aligned}$$

It remains to show that $\omega_0(\tau), \omega_1(\tau), \omega_2(\tau)$, and $\omega_3(\tau)$ are positive. The proof is trivial for $\omega_0(\tau)$. For $\omega_1(\tau)$ we use the strict convexity of $f(x) = x^{-\tau}$ together with

$$\begin{aligned} b^3 &> b^3 - b + 1 > b^3 - b^2 + b > b^3 - b^2 + 1 > b^2 - b + 1 > b > 1, \\ b^3 &> b^3 - b + 1 > b^3 - b^2 + b > b^2 > b^2 - b + 1 > b > 1 \end{aligned}$$

to apply Karamata's inequality, which gives

$$\begin{aligned} f(b^3) + f(b^2 - b + 1) &> f(b^3 - b + 1) + f(b^2) \\ &\Rightarrow b^{-3\tau} + (b^2 - b + 1)^{-\tau} > (b^3 - b + 1)^{-\tau} + b^{-2\tau} \\ &\Rightarrow \omega_1(\tau) > 0 \end{aligned}$$

and

$$\begin{aligned} f(b^3) + f(b^3 - b^2 + 1) &> f(b^3 - b + 1) + f(b^3 - b^2 + b) \\ &\Rightarrow b^{-3\tau} + (b^3 - b^2 + 1)^{-\tau} > (b^3 - b + 1)^{-\tau} + (b^3 - b^2 + b)^{-\tau} \\ &\Rightarrow \omega_2(\tau) > 0. \end{aligned}$$

For $\omega_3(\tau)$ we use the strict convexity of $f(x) = x^{-\tau} - (x + b^3 - b^2)^{-\tau}$ and apply again Karamata's inequality

$$\begin{aligned} f(b^2) + f(1) &> f(b^2 - b + 1) + f(b) \\ &\Rightarrow b^{-2\tau} - b^{-3\tau} + 1 - (1 + b^3 - b^2)^{-\tau} \\ &\quad > (b^2 - b + 1)^{-\tau} - (b^3 - b + 1)^{-\tau} + b^{-\tau} - (b^3 - b^2 + b)^{-\tau} \\ &\Rightarrow \omega_3(\tau) > 0. \end{aligned}$$

□

LEMMA 10. For a random variable r distributed according to (4), the expectation of $(g(r))^2$ with $g, \omega_0, \omega_1, \omega_2$, and ω_3 as defined in Lemma 9 can be approximated using Lemma 2 by

$$\mathbb{E}((g(r))^2) \approx \frac{m^{2\tau} \Gamma(2\tau) \ln b}{n^{2\tau} (\Gamma(\tau))^2} \frac{\eta_0^2 \omega_0(2\tau) + \eta_1^2 \omega_1(2\tau) + \eta_2^2 \omega_2(2\tau) + \eta_3^2 \omega_3(2\tau)}{(\eta_0 \omega_0(\tau) + \eta_1 \omega_1(\tau) + \eta_2 \omega_2(\tau) + \eta_3 \omega_3(\tau))^2}. \quad (27)$$

PROOF. We define $\tau' := 2\tau$ and

$$\eta'_j := \eta_j^2 \frac{(\eta_0 \omega_0(\tau) + \eta_1 \omega_1(\tau) + \eta_2 \omega_2(\tau) + \eta_3 \omega_3(\tau))^2}{\eta_0^2 \omega_0(2\tau) + \eta_1^2 \omega_1(2\tau) + \eta_2^2 \omega_2(2\tau) + \eta_3^2 \omega_3(2\tau)} \frac{(\Gamma(\tau))^2}{\Gamma(2\tau) \ln b}.$$

Since (26) implies

$$\eta'_0 \omega_0(\tau') + \eta'_1 \omega_1(\tau') + \eta'_2 \omega_2(\tau') + \eta'_3 \omega_3(\tau') = \frac{\ln b}{\Gamma(\tau')},$$

we can apply Lemma 9 giving

$$\mathbb{E}(b^{-\tau' \lfloor r/4 \rfloor} \eta'_{r \bmod 4}) \approx \frac{m^{\tau'}}{n^{\tau'}}$$

which is equivalent to

$$\mathbb{E}(b^{-2\tau \lfloor r/4 \rfloor} \eta^2_{r \bmod 4}) \cdot \frac{(\eta_0 \omega_0(\tau) + \eta_1 \omega_1(\tau) + \eta_2 \omega_2(\tau) + \eta_3 \omega_3(\tau))^2}{\eta_0^2 \omega_0(2\tau) + \eta_1^2 \omega_1(2\tau) + \eta_2^2 \omega_2(2\tau) + \eta_3^2 \omega_3(2\tau)} \frac{(\Gamma(\tau))^2}{\Gamma(2\tau) \ln b} \approx \frac{m^{2\tau}}{n^{2\tau}}$$

and finally leads to (27). \square

LEMMA 11. The approximation for $\mathbb{E}((g(r))^2)$ given in Lemma 10 is minimized for

$$\eta_j = \frac{\ln b}{\Gamma(\tau)} \frac{\omega_j(\tau)}{\omega_j(2\tau)} \left(\frac{\omega_0^2(\tau)}{\omega_0(2\tau)} + \frac{\omega_1^2(\tau)}{\omega_1(2\tau)} + \frac{\omega_2^2(\tau)}{\omega_2(2\tau)} + \frac{\omega_3^2(\tau)}{\omega_3(2\tau)} \right)^{-1} \quad (28)$$

and the corresponding minimum is given by

$$\min_{\eta_0, \eta_1, \eta_2, \eta_3} \mathbb{E}((g(r))^2) \approx \frac{m^{2\tau}}{n^{2\tau}} \frac{\Gamma(2\tau) \ln b}{(\Gamma(\tau))^2} \left(\sum_{j=0}^3 \frac{\omega_j^2(\tau)}{\omega_j(2\tau)} \right)^{-1}. \quad (29)$$

PROOF. The Cauchy-Schwarz inequality

$$\begin{aligned} & \left(\sum_{j=0}^3 \eta_j^2 \omega_j(2\tau) \right) \left(\sum_{j=0}^3 \frac{\omega_j^2(\tau)}{\omega_j(2\tau)} \right) \\ &= \left(\sum_{j=0}^3 \left(\eta_j \sqrt{\omega_j(2\tau)} \right)^2 \right) \left(\sum_{j=0}^3 \left(\frac{\omega_j(\tau)}{\sqrt{\omega_j(2\tau)}} \right)^2 \right) \\ &\geq \left(\sum_{j=0}^3 \left(\eta_j \sqrt{\omega_j(2\tau)} \right) \left(\frac{\omega_j(\tau)}{\sqrt{\omega_j(2\tau)}} \right) \right)^2 = \left(\sum_{j=0}^3 \eta_j \omega_j(\tau) \right)^2 \end{aligned}$$

gives

$$\frac{\eta_0^2 \omega_0(2\tau) + \eta_1^2 \omega_1(2\tau) + \eta_2^2 \omega_2(2\tau) + \eta_3^2 \omega_3(2\tau)}{(\eta_0 \omega_0(\tau) + \eta_1 \omega_1(\tau) + \eta_2 \omega_2(\tau) + \eta_3 \omega_3(\tau))^2} \geq \frac{1}{\sum_{j=0}^3 \frac{\omega_j^2(\tau)}{\omega_j(2\tau)}}$$

with equality for

$$\eta_0 \frac{\omega_0(2\tau)}{\omega_0(\tau)} = \eta_1 \frac{\omega_1(2\tau)}{\omega_1(\tau)} = \eta_2 \frac{\omega_2(2\tau)}{\omega_2(\tau)} = \eta_3 \frac{\omega_3(2\tau)}{\omega_3(\tau)}. \quad (30)$$

Replacing the left-hand side expression of the inequality that also appears in (27) by the corresponding right-hand side leads to the

claimed minimum (29). (30) defines the corresponding ratios between η_0, η_1, η_2 , and η_3 . Scaling those values to satisfy constraint (26) finally gives (28). \square

LEMMA 12. Consider m independent random variables r_i that are distributed according to (4) and a function $g(r)$ for which $\mathbb{E}(g(r_i)) = \frac{m^\tau}{n^\tau}$. The second-order Delta method [11] yields the estimator

$$\hat{n} = m^{1+\frac{1}{\tau}} \cdot \left(\sum_{i=0}^{m-1} g(r_i) \right)^{-\frac{1}{\tau}} \cdot \left(1 + \frac{1+\tau}{2} \frac{v}{m} \right)^{-1} \quad (31)$$

for n with relative variance

$$\text{Var}(\hat{n}) \approx \frac{v}{m} + O\left(\frac{1}{m^2}\right)$$

and

$$v = \frac{1}{\tau^2} \frac{n^{2\tau}}{m^{2\tau}} \text{Var}(g(r_i)) = \frac{1}{\tau^2} \left(\frac{n^{2\tau}}{m^{2\tau}} \mathbb{E}((g(r_i))^2) - 1 \right). \quad (32)$$

PROOF. Consider the statistic $X_m := \frac{1}{m^{1+\tau}} \sum_{i=0}^{m-1} g(r_i)$ for which $\mathbb{E}(X_m) = \frac{1}{n^\tau}$ and $\text{Var}(X_m) = \frac{v \tau^2}{m n^{2\tau}}$. The second-order Delta method gives

$$f(X_m) - f\left(\frac{1}{n^\tau}\right) \approx (X_m - \frac{1}{n^\tau}) f'\left(\frac{1}{n^\tau}\right) + \frac{1}{2} (X_m - \frac{1}{n^\tau})^2 f''\left(\frac{1}{n^\tau}\right)$$

with the transformation $f(x) := x^{-\frac{1}{\tau}}$ and its derivatives $f'(x) = -\frac{1}{\tau} x^{-\frac{1}{\tau}-1}$ and $f''(x) = \frac{1+\tau}{\tau^2} x^{-\frac{1}{\tau}-2}$. Taking the expectation on both sides gives

$$\mathbb{E}(X_m^{-\frac{1}{\tau}}) - n \approx \frac{1+\tau}{2\tau^2} \text{Var}(X_m) n^{2\tau+1} \approx n \frac{1+\tau}{2} \frac{v}{m}$$

and therefore

$$n \approx \frac{\mathbb{E}(X_m^{-\frac{1}{\tau}})}{1 + \frac{1+\tau}{2} \frac{v}{m}} = \mathbb{E} \left(m^{1+\frac{1}{\tau}} \cdot \left(\sum_{i=0}^{m-1} g(r_i) \right)^{-\frac{1}{\tau}} \cdot \left(1 + \frac{1+\tau}{2} \frac{v}{m} \right)^{-1} \right)$$

which directly leads to (31).

For the variance we use

$$(f(X_m) - f(n^{-\tau}))^2 \approx (X_m - n^{-\tau})^2 (f'(n^{-\tau}))^2$$

and again take the expectation on both sides which leads to

$$\mathbb{E}((X_m^{-\frac{1}{\tau}} - n)^2) \approx \text{Var}(X_m) (f'(n^{-\tau}))^2 = \frac{vn^2}{m}.$$

This gives for the relative variance of estimator \hat{n}

$$\begin{aligned} \text{Var}\left(\frac{\hat{n}}{n}\right) &= \frac{1}{n^2} \mathbb{E} \left(\left(\frac{1}{1 + \frac{1+\tau}{2} \frac{v}{m}} X_m^{-\frac{1}{\tau}} - n \right)^2 \right) \\ &= \frac{1}{n^2} \mathbb{E} \left(\frac{(X_m^{-\frac{1}{\tau}} - n)^2 - 2(n \frac{1+\tau}{2} \frac{v}{m})(X_m^{-\frac{1}{\tau}} - n) + (n \frac{1+\tau}{2} \frac{v}{m})^2}{(1 + \frac{1+\tau}{2} \frac{v}{m})^2} \right) \\ &\approx \frac{1}{n^2} \left(\frac{\frac{vn^2}{m} - (n \frac{1+\tau}{2} \frac{v}{m})^2}{(1 + \frac{1+\tau}{2} \frac{v}{m})^2} \right) = \frac{v}{m} \frac{1 - (\frac{1+\tau}{2})^2 \frac{v}{m}}{(1 + \frac{1+\tau}{2} \frac{v}{m})^2} = \frac{v}{m} + O\left(\frac{1}{m^2}\right). \end{aligned}$$

LEMMA 13. Let A_k be independent events that occur with probability $\Pr(A_k) = 1 - z_k$ with $z_k := e^{-\frac{n}{m^{2k}}}$. Consider $\tilde{r} = 4\tilde{u} + \langle \tilde{l}_1 \tilde{l}_2 \rangle_2$ defined by $\tilde{u} = \max\{k | A_k\}$, $\tilde{l}_1 = [A_{\tilde{u}-1}]$, and $\tilde{l}_2 = [A_{\tilde{u}-2}]$ where we used the Iverson bracket notation. Furthermore, consider $r =$

$4u + \langle l_1 l_2 \rangle_2$ defined by $u = \max(0, \min(w, \tilde{u}))$, $l_1 = [A_{u-1} \wedge u > 1]$, and $l_2 = [A_{u-2} \wedge u > 2]$ with $w \geq 3$. Then the conditional PMF of \tilde{r} for known r is given by

$$\tilde{\rho}_{\text{reg}}(\tilde{r}|r,n) = \begin{cases} \frac{z_u(1-z_u) \prod_{j=1}^2 z_{u-j}^{1-l_j} (1-z_{u-j})^{l_j}}{z_0} & r=0, \tilde{r}=4u+\langle l_1 l_2 \rangle_2, u \leq 0, \\ z_0^{1-l_1} (1-z_0)^{l_1} z_{-1}^{1-l_2} (1-z_{-1})^{l_2} & r=4, \tilde{r}=4+\langle l_1 l_2 \rangle_2, \\ z_0^{1-l_1} (1-z_0)^{l_1} & r=8, \tilde{r}=8+\langle l_1 \rangle_2, \\ z_0^{1-l_1} (1-z_0)^{l_1} & r=10, \tilde{r}=10+\langle l_1 \rangle_2, \\ 1 & 12 \leq r < 4w, \tilde{r}=r, \\ \frac{z_w(1-z_w)}{1-z_{w-1}}, & r \geq 4w, \tilde{r}=r, \\ \frac{z_{w+1}(1-z_{w+1})z_w}{1-z_{w-1}}, & r=4w+\langle l_1 l_2 \rangle_2, \tilde{r}=4w+4+l_1, \\ \frac{z_{w+1}(1-z_{w+1})(1-z_w)}{1-z_{w-1}}, & r=4w+\langle l_1 l_2 \rangle_2, \tilde{r}=4w+6+l_1, \\ \frac{z_u(1-z_u) \prod_{j=1}^2 z_{u-j}^{1-l_j} (1-z_{u-j})^{l_j}}{1-z_{w-1}} & r \geq 4w, \tilde{r}=4u+\langle l_1 l_2 \rangle_2, u \geq w+2, \\ 0 & \text{else.} \end{cases} \quad (33)$$

PROOF. The PMF of \tilde{r} is given by

$$\tilde{\rho}_{\text{reg}}(\tilde{r}|n) = \begin{cases} \Pr(\bar{A}_{u-2} \wedge \bar{A}_{u-1} \wedge A_u \wedge \bigwedge_{k=u+1}^{\infty} \bar{A}_k) & \tilde{r}=4u, \\ \Pr(\bar{A}_{u-2} \wedge \bar{A}_{u-1} \wedge A_u \wedge \bigwedge_{k=u+1}^{\infty} \bar{A}_k) & \tilde{r}=4u+1, \\ \Pr(\bar{A}_{u-2} \wedge \bar{A}_{u-1} \wedge A_u \wedge \bigwedge_{k=u+1}^{\infty} \bar{A}_k) & \tilde{r}=4u+2, \\ \Pr(\bar{A}_{u-2} \wedge \bar{A}_{u-1} \wedge A_u \wedge \bigwedge_{k=u+1}^{\infty} \bar{A}_k) & \tilde{r}=4u+3, \end{cases}$$

and that of r is given by

$$\rho_{\text{reg}}(r|n) = \begin{cases} \Pr(\bigwedge_{k=1}^{\infty} \bar{A}_k) & r=0, \\ \Pr(A_1 \wedge \bigwedge_{k=2}^{\infty} \bar{A}_k) & r=4, \\ \Pr(\bar{A}_1 \wedge A_2 \wedge \bigwedge_{k=3}^{\infty} \bar{A}_k) & r=8, \\ \Pr(A_1 \wedge A_2 \wedge \bigwedge_{k=3}^{\infty} \bar{A}_k) & r=10, \\ \Pr(\bar{A}_{u-2} \wedge \bar{A}_{u-1} \wedge A_u \wedge \bigwedge_{k=u+1}^{\infty} \bar{A}_k) & r=4u, 3 \leq u < w, \\ \Pr(\bar{A}_{u-2} \wedge \bar{A}_{u-1} \wedge A_u \wedge \bigwedge_{k=u+1}^{\infty} \bar{A}_k) & r=4u+1, 3 \leq u < w, \\ \Pr(\bar{A}_{u-2} \wedge \bar{A}_{u-1} \wedge A_u \wedge \bigwedge_{k=u+1}^{\infty} \bar{A}_k) & r=4u+2, 3 \leq u < w, \\ \Pr(A_{u-2} \wedge \bar{A}_{u-1} \wedge A_u \wedge \bigwedge_{k=u+1}^{\infty} \bar{A}_k) & r=4u+3, 3 \leq u < w, \\ \Pr(\bar{A}_{w-2} \wedge \bar{A}_{w-1} \wedge \bigvee_{k=w}^{\infty} A_k) & r=4w, \\ \Pr(A_{w-2} \wedge \bar{A}_{w-1} \wedge \bigvee_{k=w}^{\infty} A_k) & r=4w+1, \\ \Pr(\bar{A}_{w-2} \wedge \bar{A}_{w-1} \wedge \bigvee_{k=w}^{\infty} A_k) & r=4w+2, \\ \Pr(A_{w-2} \wedge \bar{A}_{w-1} \wedge \bigvee_{k=w}^{\infty} A_k) & r=4w+3, \\ 0 & \text{else.} \end{cases}$$

Using the identity $\Pr(X|Y) = \Pr(X \wedge Y)/\Pr(Y)$ and considering all cases of both PMFs gives for the PMF of \tilde{r} conditioned on r

$$\begin{aligned} & \Pr(\bar{A}_{u-2} \wedge \bar{A}_{u-1} \wedge A_u \wedge \bigwedge_{k=u+1}^0 \bar{A}_k) & r=0, \tilde{r}=4u, u \leq 0, \\ & \Pr(A_{u-2} \wedge \bar{A}_{u-1} \wedge A_u \wedge \bigwedge_{k=u+1}^0 \bar{A}_k) & r=0, \tilde{r}=4u+1, u \leq 0, \\ & \Pr(\bar{A}_{u-2} \wedge \bar{A}_{u-1} \wedge A_u \wedge \bigwedge_{k=u+1}^0 \bar{A}_k) & r=0, \tilde{r}=4u+2, u \leq 0, \\ & \Pr(A_{u-2} \wedge \bar{A}_{u-1} \wedge A_u \wedge \bigwedge_{k=u+1}^0 \bar{A}_k) & r=0, \tilde{r}=4u+3, u \leq 0, \\ & \Pr(\bar{A}_{-1} \wedge A_0) & r=4, \tilde{r}=4, \\ & \Pr(A_{-1} \wedge \bar{A}_0) & r=4, \tilde{r}=5, \\ & \Pr(\bar{A}_{-1} \wedge A_0) & r=4, \tilde{r}=6, \\ & \Pr(A_{-1} \wedge A_0) & r=4, \tilde{r}=7, \\ & \Pr(\bar{A}_0) & r=8, \tilde{r}=8, \\ & \Pr(A_0) & r=8, \tilde{r}=9, \\ & \Pr(\bar{A}_0) & r=10, \tilde{r}=10, \\ & \Pr(A_0) & r=10, \tilde{r}=11, \\ & 1 & 12 \leq r < 4w, \tilde{r}=r, \\ & \frac{\Pr(A_w \wedge \bigwedge_{k=w+1}^{\infty} \bar{A}_k)}{\Pr(\bigvee_{k=w}^{\infty} A_k)} & r=4w, \tilde{r}=4w, \\ & \frac{\Pr(A_w \wedge \bigwedge_{k=w+1}^{\infty} \bar{A}_k)}{\Pr(\bigvee_{k=w}^{\infty} \bar{A}_k)} & r=4w+1, \tilde{r}=4w+1, \\ & \frac{\Pr(A_w \wedge \bigwedge_{k=w+1}^{\infty} \bar{A}_k)}{\Pr(\bigvee_{k=w}^{\infty} \bar{A}_k)} & r=4w+2, \tilde{r}=4w+2, \\ & \frac{\Pr(\bar{A}_w \wedge \bigwedge_{k=w+1}^{\infty} \bar{A}_k)}{\Pr(\bigvee_{k=w}^{\infty} A_k)} & r=4w+3, \tilde{r}=4w+3, \\ & \frac{\Pr(\bar{A}_w \wedge A_{w+1} \wedge \bigwedge_{k=w+2}^{\infty} \bar{A}_k)}{\Pr(\bigvee_{k=w}^{\infty} A_k)} & r=4w, \tilde{r}=4w+4, \\ & \frac{\Pr(\bar{A}_w \wedge A_{w+1} \wedge \bigwedge_{k=w+2}^{\infty} \bar{A}_k)}{\Pr(\bigvee_{k=w}^{\infty} \bar{A}_k)} & r=4w+1, \tilde{r}=4w+4, \\ & \frac{\Pr(\bar{A}_w \wedge A_{w+1} \wedge \bigwedge_{k=w+2}^{\infty} \bar{A}_k)}{\Pr(\bigvee_{k=w}^{\infty} \bar{A}_k)} & r=4w+2, \tilde{r}=4w+4, \\ & \frac{\Pr(\bar{A}_w \wedge A_{w+1} \wedge \bigwedge_{k=w+2}^{\infty} \bar{A}_k)}{\Pr(\bigvee_{k=w}^{\infty} A_k)} & r=4w+3, \tilde{r}=4w+5, \\ & \frac{\Pr(\bar{A}_w \wedge A_{w+1} \wedge \bigwedge_{k=w+2}^{\infty} \bar{A}_k)}{\Pr(\bigvee_{k=w}^{\infty} \bar{A}_k)} & r=4w+4, \tilde{r}=4w+5, \\ & \frac{\Pr(\bar{A}_w \wedge A_{w+1} \wedge \bigwedge_{k=w+2}^{\infty} \bar{A}_k)}{\Pr(\bigvee_{k=w}^{\infty} \bar{A}_k)} & r=4w+5, \tilde{r}=4w+5, \\ & \frac{\Pr(\bar{A}_w \wedge A_{w+1} \wedge \bigwedge_{k=w+2}^{\infty} \bar{A}_k)}{\Pr(\bigvee_{k=w}^{\infty} A_k)} & r=4w+6, \tilde{r}=4w+6, \\ & \frac{\Pr(\bar{A}_w \wedge A_{w+1} \wedge \bigwedge_{k=w+2}^{\infty} \bar{A}_k)}{\Pr(\bigvee_{k=w}^{\infty} \bar{A}_k)} & r=4w+7, \tilde{r}=4w+6, \\ & \frac{\Pr(\bar{A}_w \wedge A_{w+1} \wedge \bigwedge_{k=w+2}^{\infty} \bar{A}_k)}{\Pr(\bigvee_{k=w}^{\infty} A_k)} & r=4w+8, \tilde{r}=4w+7, \\ & \frac{\Pr(\bar{A}_{u-2} \wedge \bar{A}_{u-1} \wedge A_u \wedge \bigwedge_{k=u+1}^{\infty} \bar{A}_k)}{\Pr(\bigvee_{k=w}^{\infty} A_k)} & r \geq 4w, \tilde{r}=4u, u \geq w+2, \\ & \frac{\Pr(\bar{A}_{u-2} \wedge \bar{A}_{u-1} \wedge A_u \wedge \bigwedge_{k=u+1}^{\infty} \bar{A}_k)}{\Pr(\bigvee_{k=w}^{\infty} \bar{A}_k)} & r \geq 4w, \tilde{r}=4u+1, u \geq w+2, \\ & \frac{\Pr(\bar{A}_{u-2} \wedge \bar{A}_{u-1} \wedge A_u \wedge \bigwedge_{k=u+1}^{\infty} \bar{A}_k)}{\Pr(\bigvee_{k=w}^{\infty} A_k)} & r \geq 4w, \tilde{r}=4u+2, u \geq w+2, \\ & \frac{\Pr(\bar{A}_{u-2} \wedge \bar{A}_{u-1} \wedge A_u \wedge \bigwedge_{k=u+1}^{\infty} \bar{A}_k)}{\Pr(\bigvee_{k=w}^{\infty} \bar{A}_k)} & r \geq 4w, \tilde{r}=4u+3, u \geq w+2, \\ & 0 & \text{else.} \end{aligned}$$

The identities

$$\begin{aligned} & \Pr(A_k) = 1 - z_k, \\ & \Pr(\bar{A}_k) = z_k, \\ & \Pr(\bigwedge_{k=u+1}^0 \bar{A}_k) = \prod_{k=u+1}^0 z_k = z_u/z_0 \quad \text{for } u \leq 0, \\ & \Pr(\bigwedge_{k=w+2}^{\infty} \bar{A}_k) = \prod_{k=w+2}^{\infty} z_k = z_{w+1}, \\ & \Pr(\bigwedge_{k=u+1}^{\infty} \bar{A}_k) = \prod_{k=u+1}^{\infty} z_k = z_u, \\ & \Pr(\bigvee_{k=w}^{\infty} A_k) = 1 - \Pr(\bigwedge_{k=w}^{\infty} \bar{A}_k) = 1 - \prod_{k=w}^{\infty} z_k = 1 - z_{w+1} \end{aligned}$$

finally lead to (33). \square

LEMMA 14. The corrected register contributions $g_{corr}(r)$ defined by

$$g_{corr}(r) = \sum_{\tilde{r}=-\infty}^{\infty} \tilde{\rho}_{reg}(\tilde{r}|r, n = \hat{n}_{alt})g(\tilde{r})$$

for $g(r) := 2^{-\tau \lfloor r/4 \rfloor} \eta_{r \bmod 4}$ and $\tilde{\rho}_{reg}$ as given by (33) results in (18).

PROOF. We use \hat{z}_0 and \hat{z}_w to denote $\hat{z}_0 := e^{-\frac{\hat{n}_{alt}}{m}}$ and $\hat{z}_w := e^{-\frac{\hat{n}_{alt}}{m^2 w}}$, respectively. The cases $r \in \{0, 4, 8, 10\}$ are shown by

$$\begin{aligned} g_{corr}(0) &= \sum_{\tilde{r}=-\infty}^{\infty} \tilde{\rho}_{reg}(\tilde{r}|0, n = \hat{n}_{alt})g(\tilde{r}) \\ &= \frac{1}{z_0} \sum_{u=-\infty}^0 \hat{z}_0^{2^{-u}} (1 - \hat{z}_0^{2^{-u}}) 2^{-\tau u} \left(\begin{array}{l} \eta_0 \hat{z}_0^{2^{-u+1}} \hat{z}_0^{2^{-u+2}} \\ + \eta_1 \hat{z}_0^{2^{-u+1}} (1 - \hat{z}_0^{2^{-u+2}}) \\ + \eta_2 (1 - \hat{z}_0^{2^{-u+1}}) \hat{z}_0^{2^{-u+2}} \\ + \eta_3 (1 - \hat{z}_0^{2^{-u+1}}) (1 - \hat{z}_0^{2^{-u+2}}) \end{array} \right) \\ &= \frac{1}{z_0} \sum_{u=0}^{\infty} 2^{\tau u} (\hat{z}_0^{2^u} - \hat{z}_0^{2^{u+1}}) \psi(\hat{z}_0^{2^{u+1}}) = \sigma(\hat{z}_0), \\ g_{corr}(4) &= \sum_{\tilde{r}=-\infty}^{\infty} \tilde{\rho}_{reg}(\tilde{r}|4, n = \hat{n}_{alt})g(\tilde{r}) \\ &= 2^{-\tau} (\eta_0 \hat{z}_0^3 + \eta_1 \hat{z}_0 (1 - \hat{z}_0^2) + \eta_2 (1 - \hat{z}_0) \hat{z}_0^2 + \eta_3 (1 - \hat{z}_0) (1 - \hat{z}_0^2)) \\ &= 2^{-\tau} \psi(\hat{z}_0), \\ g_{corr}(8) &= \sum_{\tilde{r}=-\infty}^{\infty} \tilde{\rho}_{reg}(\tilde{r}|8, n = \hat{n}_{alt})g(\tilde{r}) \\ &= 2^{-2\tau} (\eta_0 \hat{z}_0 + \eta_1 (1 - \hat{z}_0)) = 4^{-\tau} (\hat{z}_0 (\eta_0 - \eta_1) + \eta_1), \\ g_{corr}(10) &= \sum_{\tilde{r}=-\infty}^{\infty} \tilde{\rho}_{reg}(\tilde{r}|10, n = \hat{n}_{alt})g(\tilde{r}) \\ &= 2^{-2\tau} (\eta_2 \hat{z}_0 + \eta_3 (1 - \hat{z}_0)) = 4^{-\tau} (\hat{z}_0 (\eta_2 - \eta_3) + \eta_3). \end{aligned}$$

The case $12 \leq r < 4w$ is trivial. The remaining case $r = 4w + \langle l_1 l_2 \rangle_2$ is proven by

$$\begin{aligned} g_{corr}(4w + \langle l_1 l_2 \rangle_2) &= \sum_{\tilde{r}=-\infty}^{\infty} \tilde{\rho}_{reg}(\tilde{r}|4w + \langle l_1 l_2 \rangle_2, n = \hat{n}_{alt})g(\tilde{r}) \\ &= 2^{-\tau w} \frac{\hat{z}_w (1 - \hat{z}_w)}{1 - \hat{z}_w^2} \eta_{2l_1+l_2} \\ &\quad + 2^{-\tau(w+1)} \frac{\sqrt{\hat{z}_w} (1 - \sqrt{\hat{z}_w}) \hat{z}_w}{1 - \hat{z}_w^2} \eta_{l_1} \\ &\quad + 2^{-\tau(w+1)} \frac{\sqrt{\hat{z}_w} (1 - \sqrt{\hat{z}_w}) (1 - \hat{z}_w)}{1 - \hat{z}_w^2} \eta_{2+l_1} \\ &\quad + \sum_{u=w+2}^{\infty} \frac{\hat{z}_w^{2^{w-u}} (1 - \hat{z}_w^{2^{w-u}})}{2^{\tau u} (1 - \hat{z}_w^2)} \left(\begin{array}{l} \eta_0 \hat{z}_w^{2^{w-u+1}} \hat{z}_w^{2^{w-u+2}} \\ + \eta_1 \hat{z}_w^{2^{w-u+1}} (1 - \hat{z}_w^{2^{w-u+2}}) \\ + \eta_2 (1 - \hat{z}_w^{2^{w-u+1}}) \hat{z}_w^{2^{w-u+2}} \\ + \eta_3 (1 - \hat{z}_w^{2^{w-u+1}}) (1 - \hat{z}_w^{2^{w-u+2}}) \end{array} \right) \\ &= 2^{-\tau w} \frac{\hat{z}_w (1 + \sqrt{\hat{z}_w})}{(1 + \sqrt{\hat{z}_w})(1 + \hat{z}_w)} \eta_{2l_1+l_2} \\ &\quad + 2^{-\tau(w+1)} \frac{\sqrt{\hat{z}_w} \hat{z}_w}{(1 + \sqrt{\hat{z}_w})(1 + \hat{z}_w)} \eta_{l_1} \end{aligned}$$

$$\begin{aligned} &+ 2^{-\tau(w+1)} \frac{\sqrt{\hat{z}_w} (1 - \hat{z}_w)}{(1 + \sqrt{\hat{z}_w})(1 + \hat{z}_w)} \eta_{2+l_1} \\ &+ \sum_{u=0}^{\infty} \frac{(\sqrt{\hat{z}_w}^{2^{-u-1}} - \sqrt{\hat{z}_w}^{2^{-u}})}{2^{\tau(w+2+u)} (1 - \hat{z}_w^2)} \left(\begin{array}{l} \eta_0 (\sqrt{\hat{z}_w}^{2^{-u}})^3 \\ + \eta_1 (\sqrt{\hat{z}_w}^{2^{-u}}) (1 - (\sqrt{\hat{z}_w}^{2^{-u}})^2) \\ + \eta_2 (1 - \sqrt{\hat{z}_w}^{2^{-u}}) (\sqrt{\hat{z}_w}^{2^{-u}})^2 \\ + \eta_3 (1 - \sqrt{\hat{z}_w}^{2^{-u}}) (1 - (\sqrt{\hat{z}_w}^{2^{-u}})^2) \end{array} \right) \\ &= \frac{\hat{z}_w (1 + \sqrt{\hat{z}_w}) \eta_{2l_1+l_2} + 2^{-\tau} \sqrt{\hat{z}_w} (\hat{z}_w (\eta_{l_1} - \eta_{2+l_1}) + \eta_{2+l_1}) + \varphi(\sqrt{\hat{z}_w})}{2^{\tau w} (1 + \sqrt{\hat{z}_w})(1 + \hat{z}_w)}. \end{aligned}$$

□

LEMMA 15. Assume m independent and identically distributed values r_i which take the values from $\{0, 4, 8, 10\}$ with probabilities (cf. (3) for $b = 2$ and $d = 2$)

$$\Pr(r_i = 0) = z_0 = z_2^4,$$

$$\Pr(r_i = 4) = z_1 (1 - z_1) = z_2^2 (1 - z_2) (1 + z_2),$$

$$\Pr(r_i = 8) = z_2 (1 - z_2) z_1 = z_2^3 (1 - z_2),$$

$$\Pr(r_i = 10) = z_2 (1 - z_2) (1 - z_1) = z_2 (1 - z_2)^2 (1 + z_2),$$

respectively. z_u is defined as $z_u := e^{-\frac{n}{m^{2u}}}$. If the corresponding observed frequencies are c_0, c_4, c_8, c_{10} , the ML estimator for $z_0 = e^{-\frac{n}{m}}$ is given by

$$\hat{z}_0 = e^{-\frac{\hat{n}_{low}}{m}} = \left(\frac{\sqrt{\beta^2 + 4\alpha\gamma} - \beta}{2\alpha} \right)^4$$

with

$$\alpha := m + 3(c_0 + c_4 + c_8 + c_{10}),$$

$$\beta := m - c_0 - c_4,$$

$$\gamma := 4c_0 + 2c_4 + 3c_8 + c_{10}.$$

PROOF. Together with $\Pr(r_i \notin \{0, 4, 8, 10\}) = 1 - \Pr(r_i = 0) - \Pr(r_i = 4) - \Pr(r_i = 8) - \Pr(r_i = 10) = 1 - z_2$ we can write the likelihood function \mathcal{L} of the m registers as

$$\begin{aligned} \mathcal{L} &= \Pr(r_i = 0)^{c_0} \Pr(r_i = 4)^{c_4} \Pr(r_i = 8)^{c_8} \Pr(r_i = 10)^{c_{10}} \cdot \\ &\quad \cdot \Pr(r_i \notin \{0, 4, 8, 10\})^{m - c_0 - c_4 - c_8 - c_{10}} \\ &= z_2^{4c_0 + 2c_4 + 3c_8 + c_{10}} (1 - z_2)^{c_{10} + m - c_0} (1 + z_2)^{c_4 + c_{10}} \end{aligned}$$

and the log-likelihood function as

$$\begin{aligned} \ln \mathcal{L} &= (4c_0 + 2c_4 + 3c_8 + c_{10}) \ln(z_2) + (c_{10} + m - c_0) \ln(1 - z_2) \\ &\quad + (c_4 + c_{10}) \ln(1 + z_2). \end{aligned}$$

The ML estimate \hat{z}_2 for z_2 can be found by setting the first derivative

$$(\ln \mathcal{L})' = \frac{4c_0 + 2c_4 + 3c_8 + c_{10}}{z_2} + \frac{c_0 - c_{10} - m}{1 - z_2} + \frac{c_4 + c_{10}}{1 + z_2}$$

equal to 0

$$\begin{aligned} \frac{4c_0 + 2c_4 + 3c_8 + c_{10}}{\hat{z}_2} + \frac{c_0 - c_{10} - m}{1 - \hat{z}_2} + \frac{c_4 + c_{10}}{1 + \hat{z}_2} &= 0 \\ \Rightarrow \alpha \hat{z}_2^2 + \beta \hat{z}_2 - \gamma &= 0 \Rightarrow \hat{z}_2 = \frac{\sqrt{\beta^2 + 4\alpha\gamma} - \beta}{2\alpha}. \end{aligned}$$

Using the invariance property of ML estimators we can estimate $z_0 = z_2^4$ by $\hat{z}_0 = \hat{z}_2^4$, which completes the proof. □

LEMMA 16. Assume m independent and identically distributed values r_i which take the values from $\{4w, 4w+1, 4w+2, 4w+3\}$ with probabilities (cf. (3) for $b=2$ and $d=2$)

$$\begin{aligned}\Pr(r_i = 4w) &= (1 - z_{w-1})z_{w-1}z_{w-2} = (1 - z_{w-1})z_{w-1}^3, \\ \Pr(r_i = 4w+1) &= (1 - z_{w-1})z_{w-1}(1 - z_{w-2}) \\ &= (1 - z_{w-1})^2z_{w-1}(1 + z_{w-1}), \\ \Pr(r_i = 4w+2) &= (1 - z_{w-1})^2z_{w-2} = (1 - z_{w-1})^2z_{w-1}^2, \\ \Pr(r_i = 4w+3) &= (1 - z_{w-1})^2(1 - z_{w-2}) \\ &= (1 - z_{w-1})^3(1 + z_{w-1}),\end{aligned}$$

respectively. z_u is defined as $z_u := e^{-\frac{n}{m^2u}}$. If the corresponding observed frequencies are $c_{4w}, c_{4w+1}, c_{4w+2}, c_{4w+3}$, the ML estimator for $z_w = e^{-\frac{n}{m^2w}}$ is given by

$$\hat{z}_w = \sqrt{\frac{\sqrt{\beta^2 + 4\alpha\gamma} - \beta}{2\alpha}}$$

with α, β, γ

$$\begin{aligned}\alpha &:= m + 3(c_{4w} + c_{4w+1} + c_{4w+2} + c_{4w+3}), \\ \beta &:= c_{4w} + c_{4w+1} + 2c_{4w+2} + 2c_{4w+3}, \\ \gamma &:= m + 2c_{4w} + c_{4w+2} - c_{4w+3}.\end{aligned}$$

PROOF. Together with $\Pr(r_i < 4w) = 1 - \Pr(r_i = 4w) - \Pr(r_i = 4w+1) - \Pr(r_i = 4w+2) - \Pr(r_i = 4w+3) = z_{w-1}$ we can write the likelihood function \mathcal{L} of the m registers as

$$\begin{aligned}\mathcal{L} &= \Pr(r_i = 4w)^{c_{4w}} \Pr(r_i = 4w+1)^{c_{4w+1}} \Pr(r_i = 4w+2)^{c_{4w+2}} \cdot \\ &\quad \Pr(r_i = 4w+3)^{c_{4w+3}} \Pr(r_i < 4w)^{m - c_{4w} - c_{4w+1} - c_{4w+2} - c_{4w+3}} \\ &= z_{w-1}^{m+2c_{4w}+c_{4w+2}-c_{4w+3}} (1 - z_{w-1})^{c_{4w}+2c_{4w+1}+2c_{4w+2}+3c_{4w+3}} \cdot \\ &\quad \cdot (1 + z_{w-1})^{c_{4w+1}+c_{4w+3}}\end{aligned}$$

and the log-likelihood function as

$$\begin{aligned}\ln \mathcal{L} &= (m + 2c_{4w} + c_{4w+2} - c_{4w+3}) \ln(z_{w-1}) \\ &\quad + (c_{4w} + 2c_{4w+1} + 2c_{4w+2} + 3c_{4w+3}) \ln(1 - z_{w-1}) \\ &\quad + (c_{4w+1} + c_{4w+3}) \ln(1 + z_{w-1}).\end{aligned}$$

The ML estimate \hat{z}_{w-1} for z_{w-1} can be found by setting the first derivative

$$\begin{aligned}(\ln \mathcal{L})' &= \frac{m + 2c_{4w} + c_{4w+2} - c_{4w+3}}{z_{w-1}} \\ &\quad + \frac{c_{4w} + 2c_{4w+1} + 2c_{4w+2} + 3c_{4w+3}}{z_{w-1} - 1} + \frac{c_{4w+1} + c_{4w+3}}{1 + z_{w-1}}\end{aligned}$$

equal to 0

$$\begin{aligned}\frac{m + 2c_{4w} + c_{4w+2} - c_{4w+3}}{\hat{z}_{w-1}} \\ + \frac{c_{4w} + 2c_{4w+1} + 2c_{4w+2} + 3c_{4w+3}}{\hat{z}_{w-1} - 1} + \frac{c_{4w+1} + c_{4w+3}}{1 + \hat{z}_{w-1}} = 0 \\ \Rightarrow \alpha \hat{z}_{w-1}^2 + \beta \hat{z}_{w-1} - \gamma = 0 \Rightarrow \hat{z}_{w-1} = \frac{\sqrt{\beta^2 + 4\alpha\gamma} - \beta}{2\alpha}.\end{aligned}$$

Using the invariance property of ML estimators we can estimate $z_w = \sqrt{z_{w-1}}$ by $\hat{z}_w = \sqrt{\hat{z}_{w-1}}$, which completes the proof. \square

LEMMA 17. The probability that a register r_i of an ULL with m registers is changed with the next new distinct element is given by $h(r_i)$ where

$$h(r) = \begin{cases} \frac{1}{m} & r = 0, \\ \frac{1}{2m} & r = 4, \\ \frac{3}{4m} & r = 8, \\ \frac{1}{4m} & r = 10, \\ \frac{7-2l_1-4l_2}{2^u m} & r = 4u + \langle l_1 l_2 \rangle_2, 3 \leq u < w, \\ \frac{3-l_1-2l_2}{2^{w-1} m} & r = 4w + \langle l_1 l_2 \rangle_2. \end{cases}$$

PROOF. The probability that register r_i is changed is given by the probability that the register is selected which is $\frac{1}{m}$ multiplied by the probability that the register is changed by the update value k whose PMF is given by

$$\rho_{\text{update}}(k) = \begin{cases} 2^{-k} & 1 \leq k < w, \\ 2^{1-w} & k = w. \end{cases}$$

This formula corresponds to (1) with $b=2$ and truncating the maximum update value at w . If the register is still in its initial state ($r_i = 0$), any update value will change the register and therefore $h(r_i) = \frac{1}{m}$. For $r_i = 4$, any update value $k \geq 2$ will change the register which results in $h(r_i) = \frac{1}{2m}$. If $r_i = 8$, update values $k \geq 3$ or $k = 1$ will change the register leading to $h(r_i) = \frac{1}{m}(\frac{1}{2} + \frac{1}{4}) = \frac{3}{4m}$. If $r_i = 10$, update values $k \geq 3$ will change the register leading to $h(r_i) = \frac{1}{4m}$. If $r_i = 4u + \langle l_1 l_2 \rangle_2$ with $3 \leq u < w$, update values k satisfying $(k > u) \vee ((k = u-1) \wedge (l_1 = 0)) \vee ((k = u-2) \wedge (l_2 = 0))$ will change the register leading to $h(r_i) = \frac{1}{m}(\frac{1}{2^u} + \frac{1-l_1}{2^{u-1}} + \frac{1-l_2}{2^{u-2}}) = \frac{7-2l_1-4l_2}{2^u m}$. If $r_i = 4w + \langle l_1 l_2 \rangle_2$, update values k satisfying $((k = w-1) \wedge (l_1 = 0)) \vee ((k = w-2) \wedge (l_2 = 0))$ will change the register leading to $h(r_i) = \frac{1}{m}(\frac{1-l_1}{2^{w-1}} + \frac{1-l_2}{2^{w-2}}) = \frac{3-l_1-2l_2}{2^{w-1} m}$. \square

LEMMA 18. The relative variance of the martingale estimator [15, 34, 39] applied to the data structure described in Section 2 can be approximated by

$$\text{Var}(\hat{n}/n) \approx \frac{\ln(b)(1 + \frac{b-d}{b-1})}{2m}$$

if the simplified model as described in Section 2.1 can be assumed and the distinct count n as well as the number of registers m are sufficiently large.

PROOF. According to [34] the variance of the relative estimation error can be expressed as

$$\text{Var}(\hat{n}/n) = \frac{1}{n^2} \left(\left(\sum_{n'=1}^n \mathbb{E}(1/\mu(r_0, \dots, r_{m-1}) | n') \right) - n \right).$$

$\mu(r_0, \dots, r_{m-1})$ is the probability that a new distinct element triggers a state change, if the current state is given by registers r_0, \dots, r_{m-1} . The probability that a register is changed by some update value k , is given by the probability that the register was never updated with the same value or a value greater than $k+d$ before. The probability that this is the case after adding n distinct elements is given by $\Pr(\bar{A}_k \wedge \bigwedge_{u=k+d+1}^{\infty} \bar{A}_u) = z_k^{1+\frac{b-d}{b-1}}$ with $z_k = e^{-\frac{n(b-1)}{mb^k}}$.

Therefore, the probability of the expectation of $\mu(r_0, \dots, r_{m-1})$ conditioned on the distinct count n is

$$\begin{aligned}\mathbb{E}(\mu(r_0, \dots, r_{m-1})|n) &\approx \sum_{k=1}^{\infty} \rho_{\text{update}}(k) z_k^{1+\frac{b-d}{b-1}} \\ &\approx \sum_{k=1}^{\infty} (b-1) b^{-k} z_k^{1+\frac{b-d}{b-1}} \xrightarrow{n \rightarrow \infty} \sum_{k=-\infty}^{\infty} (b-1) b^{-k} z_k^{1+\frac{b-d}{b-1}} \\ &= -\frac{m}{n} \sum_{k=-\infty}^{\infty} z_k^{1+\frac{b-d}{b-1}} \ln z_k \approx \frac{m}{n} \frac{1}{\ln b} \int_0^1 z^{\frac{b-d}{b-1}} dz \\ &= \frac{m}{n} \frac{1}{\ln b} \frac{1}{1 + \frac{b-d}{b-1}}.\end{aligned}$$

Here we used Lemma 2 to approximate the sum by an integral. Since the state change probability is the sum of the individual register change probabilities, the Delta method can be used for $m \rightarrow \infty$ to approximate $\mathbb{E}(1/\mu(r_0, \dots, r_{m-1})|n)$ by

$$\begin{aligned}\mathbb{E}(1/\mu(r_0, \dots, r_{m-1})|n) &\approx \frac{1}{\mathbb{E}(\mu(r_0, \dots, r_{m-1})|n)} \\ &\approx \frac{n}{m} \ln(b) \left(1 + \frac{b-d}{b-1} \right)\end{aligned}$$

which finally leads to

$$\text{Var}(\hat{n}/n) \xrightarrow{n, m \rightarrow \infty} \frac{1}{n^2} \left(\left(\sum_{n'=1}^n \frac{n'}{m} \ln(b) \left(1 + \frac{b-d}{b-1} \right) \right) - n \right)$$

$$= \frac{1}{n^2} \frac{n(n+1)}{2m} \ln(b) \left(1 + \frac{b-d}{b-1} \right) - \frac{1}{n} \xrightarrow{n \rightarrow \infty} \frac{\ln(b)(1 + \frac{b-d}{b-1})}{2m}.$$

□

B ADDITIONAL FIGURES

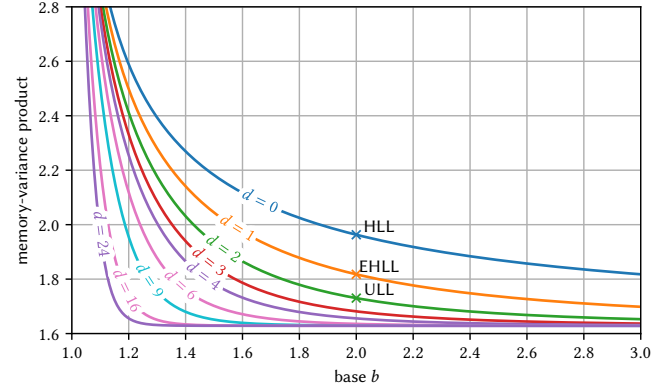


Figure 11: The theoretical asymptotic memory-variance product (MVP) over the base b for various values of d when using martingale estimation under the assumption of optimal lossless compression. The MVP of UltraLogLog (ULL) is 12% smaller than that of HyperLogLog (HLL). The theoretical limit of 1.63 [34] is reached for $b^{-d}/(b-1) \rightarrow 0$.